Equilibrium states of class-I Bragg resonant wave system

CrossMark

Dali Xu [a], Zhiliang Lin [a,*], Shijun Liao [a,b,*]

[a] *State Key Laboratory of Ocean Engineering, School of Naval Architecture, Ocean and Civil Engineering, Shanghai Jiao Tong University, Shanghai 200240, China*
[b] *Nonlinear Analysis and Applied Mathematics (NAAM) Research Group Faculty of Science, King Abdulaziz University, Jeddah 21589, Saudi Arabia*

HIGHLIGHTS

- The class-I Bragg resonant waves are solved analytically.
- Multiple equilibrium-state resonant wave systems with time-independent wave spectrum are found.
- Bifurcations with respect to wave propagation angle, water depth, bottom slope and nonlinearity are found.

ABSTRACT

In this paper, the class-I Bragg resonant waves are investigated in the case that a primary surface wave propagates obliquely over the bottom with ripples distributed in a very large area. Two kinds of equilibrium-state resonant wave systems with time-independent wave spectrum are found. In all cases, the primary and resonant wave components contain most of the wave energies. For the first kind, the primary and resonant wave components have the same amplitude. However, for the second kind, they contain different wave energies. Especially, the bifurcations of the equilibrium-state resonant waves with respect to the wave propagation angle, the water depth, bottom slope and nonlinearity are found for the first time. To the best of our knowledge, these two kinds of equilibrium-state class-I Bragg resonant waves and especially the bifurcations have never been reported. All of these might deepen and enrich our understanding about the Bragg wave resonance. Mathematically, unlike previous analytic approaches which regard the considered problem as an initial-value one, we search for the unknown equilibrium-state resonant waves from the viewpoint of boundary-value problem, using an analytic method that has nothing to do with small/large physical parameters at all.

© 2014 Elsevier Masson SAS. All rights reserved.

1. Introduction

In his pioneering work, Phillips [1] found the resonance criterion of a quartet of progressive waves in deep water:

$$\boldsymbol{k}_1 \pm \boldsymbol{k}_2 \pm \boldsymbol{k}_3 \pm \boldsymbol{k}_4 = 0, \qquad \omega_1 \pm \omega_2 \pm \omega_3 \pm \omega_4 = 0, \qquad (1)$$

where $\boldsymbol{k}_i$ denotes the wave number, $\omega_i = \sqrt{gk_i}$ with $k_i = |\boldsymbol{k}_i|$ being the angular frequency given by the linear wave theory in deep water, g is the acceleration due to gravity, respectively. Phillips [1] found that the amplitude of the resonant wave component, if it is zero initially, grows linearly with time. When Phillips' resonance criterion (1) is fully or nearly satisfied, Benney [2] established the evolution equations of wave mode amplitudes, and demonstrated

the well-known time-dependent periodic exchanges of wave energy governed by Jacobian elliptic functions.

Same as the Stokes wave [3–5], there were some attempts to obtain the equilibrium states of this quartet resonance with the *time-independent* wave amplitude, angular frequency and wavenumber. In the context of perturbation techniques, the equilibrium states of the quartet resonance have *not* been found at an order higher than three, because perturbation results (mostly at the third order of approximation) contain the secular terms when Phillips' criterion is satisfied so that "the perturbation theory breaks down due to singularities in the transfer functions", as currently pointed out by Madsen and Fuhrman [6]. However, using an analytic approximation method for highly nonlinear problems, namely the homotopy analysis method (HAM) [7–13], Liao [14] successfully gained, for the first time, the equilibrium states of the quartet resonant progressive waves in deep water, which have no exchange of wave energy at all between different wave components. In addition, Liao [14] found that there exist multiple equilibrium states

---

of this quartet resonance in deep water, and especially the resonant wave component may contain much *less* wave energy than the primary ones.

Based on the homotopy, a basic concept of topology, the HAM has many advantages over other analytic approximation techniques for nonlinear problems. First, unlike perturbation techniques, it has nothing to do with small/large physical parameters, and thus is valid for more problems in science and engineering. Besides, it provides us great freedom to choose the base-function and equation-type of equations for high-order approximations. Especially, different from all other analytic approximation methods, the HAM provides us a simple, convenient way to guarantee the convergence of solution series. In addition, the HAM has been proved to logically include some traditional analytic approximation methods, such as "the Lyapunov artificial small parameter method" proposed by the famous Russian mathematician Aleksandr Mikhailovich Lyapunov (1857–1918), "the Adomian decomposition method" which was developed from the 1970s to the 1990s by George Adomian, the chair of the Center for Applied Mathematics at the University of Georgia, USA, and so on. Thus, the HAM has rather general meanings in theory. The HAM has been successfully applied to solve many nonlinear problems in fluid mechanics, applied mathematics, physics, finance and so on. Especially, some new solutions were found by means of the HAM, which had never been reported and neglected by other analytic approximation methods and even by numerical techniques. All of these illustrate the validity and novelty of the HAM. For details about the HAM, please refer to the two books of Liao [8,11]. It should be emphasized that the multiple equilibrium states of resonant wave systems in deep water were first discovered by Liao [14] using the HAM.

In 2012, Xu et al. [15] further applied the HAM to solve this quartet resonance of progressive waves in *finite* water depth d with flat bottom, when Phillips' resonance criterion (1) with $\omega_i = \sqrt{gk_i \tanh k_i d}$ is exactly satisfied. They confirmed that the multiple equilibrium states of resonant waves also exist in finite water depth. Meanwhile, the resonant wave component might contain a small proportion of wave energy, too. Besides, they verified all of their conclusions using the Zakharov equation. In addition, Liu et al. [16] verify that the multiple equilibrium states also exist in the resonance of multiple waves. Current, Liu et al. [17] confirmed the existence of the steady-state resonant waves by experiments: their experimental results agree quite well with the theoretical ones reported in [16]. All of these confirmed the generality of the multiple equilibrium-states of resonant wave systems in deep and finite water.

A simple pendulum without damping, as plotted in Fig. 1, is a good analogy for the equilibrium-states of resonant wave systems. When the pendulum is at the lowest position initially, it will stay at this equilibrium position forever. When the pendulum is disturbed away from this equilibrium position, it oscillates periodically around it, with the periodic exchange of its potential energy and kinetic energy. Thus, equilibrium-states of a dynamic system are fundamental and important for us to have a global understanding of it. Some complicated dynamic systems have multiple equilibrium positions. The resonant waves as dynamical systems are much more complicated than a simple pendulum: they have multiple equilibrium states. The equilibrium states of the resonant wave systems found by Liao [14] in deep water and Xu et al. [15] in finite water depth are like the equilibrium positions of a complicated dynamical system. Such kind of equilibrium states determine the global characteristics of the dynamic system and thus belong to a kind of fundamental property. Therefore, it is very important to determine these equilibrium states of resonant waves, which are helpful to deepen and enrich our understandings about resonant waves. Note that such kind of equilibrium states are rather special
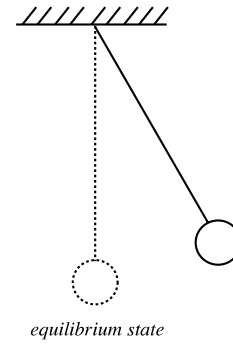

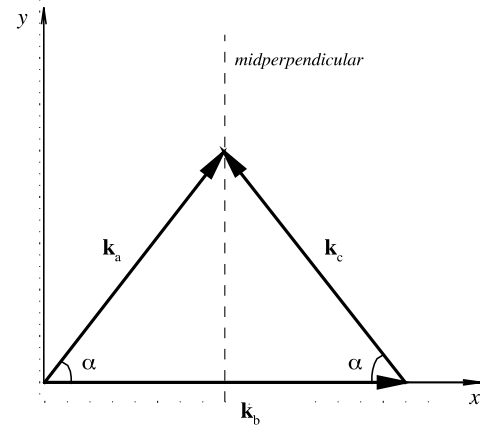**Fig. 1.** Equilibrium state of dynamical systems.

Fig. 2. Sketch map of the class-I Bragg resonant waves.

in practice. In most cases, there often exist the time-dependent periodic exchanges of wave energy around these equilibrium states, which can be described by the evolution equations of wave mode amplitudes given by Benney [2]. However, Benney [2] did not report the existence of the multiple equilibrium states of resonant waves, which were first found by Liao [14] in deep water, confirmed by Xu et al. [15] in water of finite depth and Liu et al. [16] for multiple wave interactions by means of the HAM.

Therefore, the equilibrium states of resonant waves are important in physics for a better understanding of global characteristic of a given resonant wave system. Do multiple equilibrium states of resonant wave systems exist generally in other more complicated cases? The answer is positive, as revealed in this article.

It is well-known that the resonance occurs for nonlinear wave–bottom interaction, too. The simplest case is known as the class-I Bragg resonance. It occurs when a primary surface wave propagates over an undulated bed that contains ripples with a single wavenumber $\boldsymbol{k}_B$. Without loss of generality, let $\boldsymbol{k}_A$ denote the wavenumber of the primary wave and $\boldsymbol{k}_C$ that of the resonant one, respectively. Note that the names of the so-called primary and resonant waves can be interchanged, since there exists a kind of symmetry on the perpendicular bisector of the bottom wavenumber $\boldsymbol{k}_B$, as shown in Fig. 2 and illustrated later. So, without loss of generality, we can simply call them wave A and wave C, too.

The corresponding class-I Bragg resonance criterion reads

$$\boldsymbol{k}_A - \boldsymbol{k}_B = \boldsymbol{k}_C, \qquad \omega_A = \omega_C, \qquad (2)$$

where

$$\omega_A = \sqrt{g|\boldsymbol{k}_A| \tanh |\boldsymbol{k}_A|d}, \qquad \omega_C = \sqrt{g|\boldsymbol{k}_C| \tanh |\boldsymbol{k}_C|d}$$

denote the wave angular frequency in the linear theory and d is the water depth, respectively. The resonant wave results from the resonant interaction between the primary wave and the bottom.

This criterion is derived from Phillips' criterion (1) at a lower order when the bottom is fixed (say, $\omega_B = 0$). The resonance criterion (2) reveals

$$|\boldsymbol{k}_A| = |\boldsymbol{k}_C| = k,$$

i.e. both of the wave A and the wave C have the same wave number, denoted by k. Meanwhile,

$$|\boldsymbol{k}_B| = 2|\boldsymbol{k}_A| \cos \alpha = 2\,k \cos \alpha, \tag{3}$$

as shown by Fig. 2, where α is the angle between the wavenumber $\boldsymbol{k}_A$ and the x-axis, since $\boldsymbol{k}_B$ is assumed in the x-axis direction.

The class-I Bragg resonance has been studied a lot in the past decades. Heathershaw [18] did an experiment when an incident wave normally propagates over a *patch* of fixed sinusoidal ripples and the class-I Bragg resonance occurs. In this experiment, the amplitude of the resonant wave component was zero initially beyond the rippled patch, and grew linearly with the propagation distance over the ripples. Several studies [19–24] have verified this result in theory.

Using the multiple scale perturbation method, Mei [25] solved the *linearized* governing equations when an incident wave over a bottom with *finite* ripples was slightly detuned from the Bragg resonance. In the so-called "perfect tuning" case, the two dimensional theoretical results of Mei [25] agree well with the experiment of Heathershaw [18]. According to Mei [25], the transmission coefficient $T(x)$ and the reflection coefficient $R(x)$ are given by

$$T(x) = \frac{A}{A_0} = \frac{\cosh \frac{\Omega_0}{C_g}(L-x)}{\cosh \frac{\Omega_0 L}{C_g}},$$

$$R(x) = \frac{B}{A_0} = \frac{-i \sinh \frac{\Omega_0}{C_g}(L-x)}{\cosh \frac{\Omega_0 L}{C_g}}, \quad 0 < x < L, \tag{4}$$

respectively, where A_0 is the wave amplitude of the incident wave beyond the rippled patch ($x < 0$), A and B are the wave amplitudes of the transmission and reflection wave modes over the ripples in a finite interval $0 < x < L$. Thus, as the interval of ripples tends to infinity, i.e. $L \to +\infty$, the ratio of amplitudes of these two components reads

$$\lim_{L \to \infty} \left| \frac{B}{A} \right| = \lim_{L \to \infty} \left| -i \tanh \frac{\Omega_0}{C_g}(L-x) \right| = 1, \tag{5}$$

which reveals that the reflection and transmission wave components have the same amplitude. In addition, Mei [25] considered the oblique incidence of slightly detuned wave propagating over the infinite ripples as well and the ratio of amplitudes of these two components is given by

$$R = \frac{B}{A} = \frac{\cos^2 \alpha}{\cos 2\alpha} \left\{ \frac{\Omega}{\Omega_0} - \left[\left(\frac{\Omega}{\Omega_0} \right)^2 - \left(\frac{\cos 2\alpha}{\cos^2 \alpha} \right)^2 \right]^{\frac{1}{2}} \right\}, \tag{6}$$

which leads to

$$|R| = 1 \quad \text{when } \Omega = 0, \tag{7}$$

i.e. the reflection and transmission wave components have the same wave amplitude and thus share the same wave energy, where α is the angle between the x-axis and the reflection/transmission wave component. Note that multiple resonant waves were *not* reported in this case [25], mainly because the *linearized* governing equations were solved. Notice that the so-called reflection and transmission wave components in the paper of Mei [25] correspond to the resonant and primary components of the equilibrium-states of the class-I Bragg resonant waves, since the wave spectrum in the equilibrium-state is time-independent so that there is no evolution of wave amplitude and frequency.

In addition, Ardhuin and Herbers [26] considered the Bragg scattering when the surface waves are random and non-stationary, propagating over a finite patch of sinusoidal bars. Further, the problem of random waves propagating over random bottom was investigated by Ardhuin and Magne [27] and the effect of current was studied as well. Yu and Mei [28] studied the coupled evolution of bars and waves through Bragg scattering. And later the linear waves propagating over periodic topographies of arbitrary amplitude and wave form was studied by Yu and Howard [29]. However, none of them obtained the equilibrium states and especially the bifurcations for the Bragg resonance.

In this paper, we investigate the class-I Bragg resonance about the nonlinear interaction between the obliquely surface wave and the bottom with ripples. When the bottom ripples are distributed in a very large area, for the sake of simplicity, we can approximately consider the bottom with an *infinite* number of ripples. Mitra and Greenberg [30] solved the same problem by regarding it as an initial value problem, and found slowly periodic energy exchanges between the wave A and the wave C. They did not report any multiple resonant waves, since an initial value problem has only one solution. Their work agreed with that of Benney [2] for surface resonant waves. Davies [31] applied perturbation method to search for equilibrium states of the class-I Bragg resonant waves, but failed, mainly because "the perturbation theory breaks down due to singularities in the transfer functions", as currently also pointed out by Madsen and Fuhrman [6]. In this paper, we successfully obtain two equilibrium states of the class-I Bragg resonant wave by means of the homotopy analysis method (HAM) [7–13]. One of them is similar to that reported by Mei [25], whose primary wave has the same wave energy as the resonant wave. However, the other does not process such kind of equality and has never been reported, say, the primary and resonant waves have different wave amplitudes. In addition, the effects of propagation angle, water depth, bottom slope and nonlinearity on the equilibrium states of the class-I Bragg resonant waves are investigated in details, and the bifurcations of the equilibrium-states solutions with respect to these physical parameters are found, for the first time, to the best of our knowledge.

This paper is organized as follows. The mathematical description of the problem is given in Section 2. The solution procedure in the context of the HAM is described in Section 3. The multiple equilibrium states of the resonant wave system in a particular case are described as an example in Section 4. The effects of the propagation angle, water depth, bottom slope and nonlinearity on the equilibrium state of the class-I Bragg resonant wave system are presented in Section 5. The bifurcations of the equilibrium states are reported in this section, too. Concluding remarks and discussions are provided in Section 6. For the sake of simplicity, the detailed mathematical formulas are given in the Appendix.

2. Mathematical description

2.1. Fully nonlinear wave equations

Let us consider the propagation of progressive waves in water of a finite depth d over a fixed bed with ripples in a sinusoidal form. When the ripples are distributed in a very large domain, infinite number of ripples are approximately considered, as depicted by Fig. 3. Assume that the fluid is inviscid and incompressible, the flow is irrotational, and the surface tension is negligible. Let (x, y) and z be the horizontal and vertical coordinates, with the x-axis in the direction of the wavenumber $\boldsymbol{k}_B$ of the bottom ripples and the z-axis upward, t denote the time, $\varsigma(x, y, t)$ the unknown wave elevation moving around the mean free surface $z = 0$, and $z = -d + \zeta(x)$ the varying bottom with a constant mean depth d,
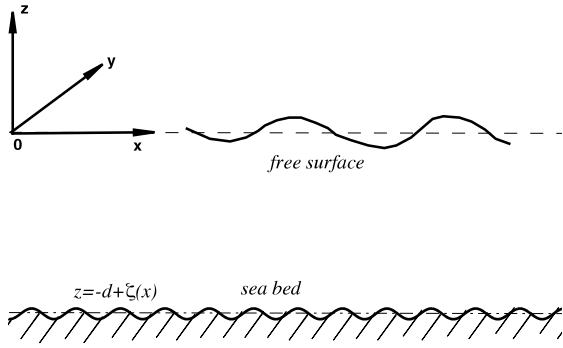
Fig. 3. Physical model.

respectively. The velocity potential $\phi(x, y, z, t)$ is governed by the Laplace equation

$$\nabla^2\phi = 0, \quad -d + \zeta(x) < z < \varsigma(x, y, t), \tag{8}$$

where

$$\nabla = \mathbf{i}\frac{\partial}{\partial x} + \mathbf{j}\frac{\partial}{\partial y} + \mathbf{k}\frac{\partial}{\partial z} \tag{9}$$

with $\mathbf{i}$, $\mathbf{j}$, $\mathbf{k}$ denoting unit vectors in the x, y, z directions, respectively. The bottom kinematical condition reads

$$\phi_z - \zeta_x\phi_x = 0, \quad \text{on } z = -d + \zeta(x), \tag{10}$$

where the bottom profile

$$\zeta(x) = b\cos(k_B x), \quad k_B = |\mathbf{k}_B|, \tag{11}$$

is given, $\mathbf{k}_B$ denotes the wavenumber of the periodic ripples in sinusoidal form on the bottom, b is the amplitude of bottom undulation, respectively. On the unknown free surface $z = \varsigma(x, y, t)$, the kinematical condition is

$$\varsigma_t - \phi_z + (\phi_x\varsigma_x + \phi_y\varsigma_y) = 0, \quad \text{on } z = \varsigma(x, y, t) \tag{12}$$

and the dynamical condition reads

$$\varsigma = -\frac{1}{g}\left(\phi_t + \frac{1}{2}\nabla\phi\cdot\nabla\phi\right), \quad \text{on } z = \varsigma(x, y, t). \tag{13}$$

On the free surface $z = \varsigma(x, y, t)$, the kinematic condition (12) and dynamical condition (13) can be combined into the fully nonlinear equation

$$\phi_{tt} + g\phi_z + 2\nabla\phi\cdot\nabla\phi_t + \frac{1}{2}\nabla\phi\cdot\nabla(\nabla\phi\cdot\nabla\phi) = 0,$$
$$\text{on } z = \varsigma(x, y, t), \tag{14}$$

which we actually solve. In addition, the resonance criterion (2) must be satisfied. The above fully nonlinear wave equations can be found in textbooks. For details, please refer to Mei et al. [32].

2.2. Dimensionless equations

Let us consider the wave A, with the wavenumber $\mathbf{k}_A = \{k\cos\alpha, k\sin\alpha\}$ and the actual frequency σ_A, where α denotes the angle between $\mathbf{k}_A$ and the x-axis with $k = |\mathbf{k}_A|$, as depicted by Fig. 2. Write

$$\epsilon = \frac{\sigma_A}{\omega_A}, \tag{15}$$

where $\omega_A = \sqrt{gk\tanh(kd)}$ is the frequency given by the linear wave theory. Since the surface condition (14) considered in this paper includes the nonlinear terms, here we have $\epsilon > 1$. Using the dimensionless variables (denoted by primes)

$$(x', y', z', d') = k(x, y, z, d), \quad t' = \sigma_A t,$$
$$\eta' = \frac{\eta}{d}, \quad \zeta' = \frac{\zeta}{b}, \quad \phi' = \frac{k\,\phi}{\sigma_A d}, \tag{16}$$

the governing equation and all boundary conditions in Section 2.1 can be rewritten in dimensionless form. For brevity, the prime (′) is omitted and all variables are dimensionless hereinafter. In this way, we have the dimensionless governing equation

$$\nabla^2\phi = 0, \quad -\epsilon_1 + (\epsilon_2/\epsilon_3)\zeta < z < \epsilon_1\varsigma, \tag{17}$$

subject to the two boundary conditions on the unknown free surface $z = \epsilon_1\varsigma(x, y, t)$,

$$\phi_{tt} + \frac{1}{\epsilon^2\tanh(\epsilon_1)}\phi_z + 2\epsilon_1\nabla\phi\cdot\nabla\phi_t$$
$$+ \frac{\epsilon_1^2}{2}\nabla\phi\cdot\nabla(\nabla\phi\cdot\nabla\phi) = 0, \tag{18}$$

$$\varsigma = -\epsilon^2\tanh(\epsilon_1)\left(\phi_t + \frac{\epsilon_1}{2}\nabla\phi\cdot\nabla\phi\right), \tag{19}$$

and the bottom condition

$$\phi_z - (\epsilon_2/\epsilon_3)\zeta_x\phi_x = 0, \quad \text{on } z = -\epsilon_1 + (\epsilon_2/\epsilon_3)\zeta, \tag{20}$$

respectively, where $\epsilon_1 = kd$, $\epsilon_2 = bk_B$ and $\epsilon_3 = k_B/k$ are three dimensionless parameters. Note that ϵ_1 denotes the dimensionless water depth, ϵ_2 the bottom slope, and ϵ_3 the ratio of the wavelength of the wave A to that of the periodically undulate bottom, respectively. According to (3), it holds $\epsilon_3 = 2\cos\alpha$ for the class-I Bragg resonance. It should be emphasized that, in the frame of the HAM, all of these three parameters ϵ_1, ϵ_2 and ϵ_3 are *unnecessary* to be small or large, as shown below.

2.3. Equations in the equilibrium state

Traditionally, the above-mentioned class-I Bragg resonant wave system was solved as an initial value problem, and the corresponding wave evolutions from the beginning at $t = 0$ were studied, as illustrated by Mei, Mitra and Greenberg [25,30]. According to Benney [2], *randomly* given an initial condition satisfying the resonance criterion, each component of the corresponding resonant wave system has mostly a periodic amplitude and frequency so that there exist the periodic exchange of wave energy. Thus, from the viewpoint of an initial value problem, the corresponding initial conditions for an equilibrium-state resonant wave system with time-independent amplitude and frequency are rather special and thus must be *unknown*, which however can be determined by means of the HAM as described below.

Different from the traditional approaches, we concentrate on the unknown equilibrium-state of the resonant wave system, whose wave amplitudes and frequencies are time-independent. Following the strategy of Liao [14] in deep water and Xu et al. [15] in finite water depth, we first assume that the equilibrium-state of the resonant wave system exists and then try to find such kind of resonant wave system. If the equilibrium-state of the resonant wave system is found, then the assumption is right. Otherwise, there is no equilibrium-state of such kind of resonant wave systems in a given case.

Since the equilibrium-state of the resonant wave system has time-independent wave amplitudes and frequencies, we can transfer the original initial-value problem (17)–(20) to a boundary-value problem by defining the two new variables

$$\xi_1 = \mathbf{k}_A\cdot\mathbf{r} - t = x\cos\alpha + y\sin\alpha - t,$$
$$\xi_2 = \mathbf{k}_B\cdot\mathbf{r} = \epsilon_3\,x, \tag{21}$$

where $\mathbf{r} = x\mathbf{i} + y\mathbf{j}$. Then, the governing equation (17) becomes

$$\phi_{\xi_1\xi_1} + 2\epsilon_3 \cos\alpha\, \phi_{\xi_1\xi_2} + \epsilon_3^2\, \phi_{\xi_2\xi_2} + \phi_{zz} = 0,$$
$$-\epsilon_1 + (\epsilon_2/\epsilon_3) \cos\xi_2 < z < \epsilon_1\eta(\xi_1, \xi_2), \tag{22}$$

subject to the two free surface boundary conditions on $z = \epsilon_1\eta(\xi_1, \xi_2)$,

$$\phi_{\xi_1\xi_1} + \frac{1}{\epsilon^2 \tanh(\epsilon_1)}\phi_z - 2\epsilon_1 f_{\xi_1} + \epsilon_1^2 \nabla\phi \cdot \nabla f = 0, \tag{23}$$

$$\eta = \epsilon^2 \tanh(\epsilon_1) \left(\phi_{\xi_1} - \epsilon_1 f\right), \tag{24}$$

and the bottom condition on $z = -\epsilon_1 + (\epsilon_2/\epsilon_3) \cos\xi_2$, i.e.

$$\phi_z + \epsilon_2 \sin\xi_2 \left(\cos\alpha\, \phi_{\xi_1} + \epsilon_3\, \phi_{\xi_2}\right) = 0, \tag{25}$$

where

$$f = \frac{1}{2}\nabla\phi \cdot \nabla\phi = \frac{1}{2}\left(\phi_{\xi_1}^2 + \epsilon_3^2\,\phi_{\xi_2}^2 + 2\epsilon_3 \cos\alpha\, \phi_{\xi_1}\phi_{\xi_2} + \phi_z^2\right). \tag{26}$$

Note that Eqs. (22)–(25) for the equilibrium-state of resonant waves with the *unknown* primary and resonant wave components (i.e. the wave A and wave C) define a nonlinear boundary-value problem, since the time t does not appear explicitly. It is well-known that nonlinear boundary-value problems often have multiple solutions. This is the mathematical reason why there exist the multiple equilibrium-states of the class-I Bragg resonant wave system.

3. Approach based on homotopy analysis method

In this section, the equilibrium state of the class-I Bragg resonance governed by the nonlinear boundary-value Eqs. (22)–(25) are solved by means of the HAM [7–13], when the resonant condition (2) is exactly satisfied. The system of the coupled nonlinear partial differential equations (PDEs) defined above can be solved by means of the HAM in a similar way to that for the equilibrium-state resonant waves in deep and finite water depth, as illustrated by Liao [14] and Xu et al. [15]. For the sake of simplicity, we only briefly describe the approach based on the HAM. The detailed mathematical formulas are given in the Appendix.

Similar to the equilibrium states of the wave–wave resonant interactions [14,15], the wave elevation of the equilibrium state of the class-I Bragg resonance can be expressed by

$$\eta(\xi_1, \xi_2) = \sum_{m=0}^{+\infty}\sum_{n=-\infty}^{+\infty} a_{m,n} \cos(m\xi_1 + n\xi_2), \tag{27}$$

where $a_{m,n}$ is a time-independent constant to be determined, i.e. $da_{m,n}/dt = 0$, since there is no wave energy exchange, and wave amplitudes and frequencies are time-independent. Here, ξ_1 and ξ_2 are defined by (21). This is because the class-I Bragg resonant waves are consist of the primary wave, the resonant wave, the periodic bottom ripples, and their nonlinear interactions. The above expression is complete, since due to (2) it holds

$$\boldsymbol{k}_C \cdot \boldsymbol{r} - t = (\boldsymbol{k}_A - \boldsymbol{k}_B) \cdot \boldsymbol{r} - t = \xi_1 - \xi_2,$$

say, the resonant wave component can be simply expressed by $a_{1,-1} \cos(\xi_1 - \xi_2)$, where $a_{1,-1}$ is a time-independent constant. So, the wave elevation of the class-I Bragg, fully resonant waves can be completely expressed by (27).

Due to the linear governing equation (22), the velocity potential $\phi(\xi_1, \xi_2, z)$ has the form

$$\phi(\xi_1, \xi_2, z) = \sum_{m=1}^{+\infty}\sum_{n=-\infty}^{+\infty} \left[b_{m,n}\Psi_{m,n} + c_{m,n} F_{m,n}\right], \tag{28}$$

with the definitions

$$\Psi_{m,n} = \sin(m\xi_1 + n\xi_2)\frac{\cosh\left[P_{m,n}(z + \epsilon_1)\right]}{\cosh(P_{m,n}\,\epsilon_1)}, \tag{29}$$

$$F_{m,n} = \sin(m\xi_1 + n\xi_2)\frac{\sinh(P_{m,n}\,z)}{P_{m,n}\cosh\left(P_{m,n}\,\epsilon_1\right)}, \tag{30}$$

$$P_{m,n} = \sqrt{m^2 + n(m+n)\,\epsilon_3^2}, \tag{31}$$

where $b_{m,n}$ and $c_{m,n}$ are time-independent constants to be determined, i.e. $db_{m,n}/dt = dc_{m,n}/dt = 0$. Note that the velocity potential (28) satisfies the linear governing equation (22) *automatically*. Thus, our aim is to obtain the wave elevation $\eta(\xi_1, \xi_2)$ in the form (27) and the velocity potential $\phi(\xi_1, \xi_2, z)$ in the form (28), which satisfy the three boundary conditions (23)–(25) with the resonant criterion (2).

In the frame of the HAM, the Mth-order approximations read

$$\phi(\xi_1, \xi_2, z) \approx \sum_{m=0}^{M} \phi_m(\xi_1, \xi_2, z), \tag{32}$$

$$\eta(\xi_1, \xi_2) \approx \sum_{m=0}^{M} \eta_m(\xi_1, \xi_2), \tag{33}$$

where $\phi_m(\xi_1, \xi_2, z)$ and $\eta_m(\xi_1, \xi_2)$ are governed by the so-called high-order deformation equations

$$\frac{\partial^2 \phi_m}{\partial\xi_1^2} + 2\epsilon_3 \cos\alpha \frac{\partial^2\phi_m}{\partial\xi_1\partial\xi_2} + \epsilon_3^2 \frac{\partial^2\phi_m}{\partial\xi_2^2} + \frac{\partial^2\phi_m}{\partial z^2} = 0,$$
$$-\epsilon_1 < z < 0, \tag{34}$$

subject to the free surface boundary condition

$$\bar{\mathcal{L}}_1[\phi_m] = R_{1,m}(\xi_1, \xi_2), \quad \text{on } z = 0 \tag{35}$$

and the bottom condition

$$\bar{\mathcal{L}}_2[\phi_m] = R_{2,m}(\xi_1, \xi_2), \quad \text{on } z = -\epsilon_1, \tag{36}$$

where

$$R_{1,m}(\xi_1, \xi_2) = c_0 \Delta_{m-1}^{\phi} + \chi_m S_{m-1} - \bar{S}_m,$$
$$R_{2,m}(\xi_1, \xi_2) = c_0 \Delta_{m-1}^{b} + \chi_m T_{m-1} - \bar{T}_m$$

are dependent upon $\phi_0, \phi_1, \dots, \phi_{m-1}$ and thus are always known. Here,

$$\bar{\mathcal{L}}_1[\phi_m] = \left.\left(\frac{\partial^2\phi_m}{\partial\xi_1^2} + \frac{1}{\tanh(\epsilon_1)}\frac{\partial\phi_m}{\partial z}\right)\right|_{z=0},$$
$$\bar{\mathcal{L}}_2[\phi_m] = \left.\frac{\partial\phi_m}{\partial z}\right|_{z=-\epsilon_1} \tag{37}$$

are two auxiliary linear operators which we have great freedom to choose. Meanwhile, we have

$$\eta_m(\xi_1, \xi_2) = c_0 \Delta_{m-1}^{\eta} + \chi_m \eta_{m-1} = R_{3,m}(\xi_1, \xi_2), \quad \text{on } z = 0, \tag{38}$$

where the function $R_{3,m}(\xi_1, \xi_2)$ is dependent upon $\phi_0, \phi_1, \dots, \phi_{m-1}$ and thus is known as well. The detailed derivation of Eqs. (35)–(38) and the explicit expressions of $R_{i,m}(\xi_1, \xi_2)(i = 1, 2, 3)$ are given in the Appendix.

Note that the auxiliary linear operator $\bar{\mathcal{L}}_1$ defined by (37) has the property

$$\bar{\mathcal{L}}_1[\Psi_{m,n}] = \lambda_{m,n} \sin(m\xi_1 + n\xi_2), \tag{39}$$

where

$$\lambda_{m,n} = \frac{P_{m,n} \tanh(P_{m,n}\,\epsilon_1)}{\tanh(\epsilon_1)} - m^2 \tag{40}$$

is the eigenvalue of $\bar{\mathcal{L}}_1$, and $P_{m,n}$ is defined by (31). Note that it holds

$$\lambda_{1,0} \equiv 0, \qquad \bar{\mathcal{L}}_1[\Psi_{1,0}] = 0 \tag{41}$$

for the wave A (with wavenumber $\boldsymbol{k}_A$). Especially, when the class-I Bragg resonance occurs, we have

$$\lambda_{1,-1} = 0, \qquad \bar{\mathcal{L}}_1[\Psi_{1,-1}] = 0 \tag{42}$$

for the wave C (with wavenumber $\boldsymbol{k}_C$), too. Thus, for the class-I Bragg resonance, the high-order deformation Eq. (35) has two homogeneous solutions, i.e. $\Psi_{1,0}$ and $\Psi_{1,-1}$. Thus, since the HAM provides us the great freedom to choose the initial guess solution, we choose the initial guess

$$\phi_0(\xi_1, \xi_2, z) = A_0^{1,0} \Psi_{1,0} + A_0^{1,-1} \Psi_{1,-1}, \tag{43}$$

where $A_0^{1,0}$ and $A_0^{1,-1}$ are time-independent constants, which are determined by two coupled nonlinear algebra equations for avoiding the so-called "secular terms" different from the solution expressions (27) and (28). In this way, the multiple equilibrium states of the class-I Bragg resonant waves can be found, and besides the singularity occurred in the perturbation approaches [31] can be avoided, as illustrated below in details.

4. Equilibrium-state resonant waves

In this section, we illustrate in details how to find the equilibrium-state class-I Bragg resonant waves using the HAM-based approach mentioned above. Without loss of generality, let us consider such a case

$$\alpha = 70°, \qquad \epsilon_1 = kd = 2.5, \qquad \epsilon_2 = bk_B = 0.005,$$
$$\epsilon = \frac{\sigma_A}{\omega_A} = \frac{\sigma_C}{\omega_C} = 1.0003. \tag{44}$$

Here we choose ϵ to be slightly larger than unity, since we consider the nonlinear effect in the surface boundary condition (14). But the value is small mainly because the frequency $\omega_A = \omega_C$ in the resonance criterion (2) is given by the linear wave theory. It should be emphasized that the class-I Bragg resonant waves are fully resonating because they satisfy

$$\boldsymbol{k}_A - \boldsymbol{k}_C - \boldsymbol{k}_B = 0, \qquad \omega_A - \omega_C = 0, \qquad \sigma_A - \sigma_C = 0. \tag{45}$$

In other words, the resonance criterion is satisfied even using the actual frequencies of wave. For the class-I Bragg resonant waves, we have due to (3) that

$$\epsilon_3 = k_B/k = 2\cos\alpha = 0.68404.$$

Thus, the shape of bottom ripple is completely fixed by the two given parameters ϵ_2 and ϵ_3. In other words, only the amplitudes of all wave components are unknown up to now.

When $m = 1$, it is straightforward to gain $\eta_1(\xi_1, \xi_2)$ by means of (38), which is dependent upon the initial guess ϕ_0 only. However, ϕ_0 contains two unknown constants $A_0^{1,0}$ and $A_0^{1,-1}$, which should be determined when solving ϕ_1, as shown below.

Substituting the initial guess (43) of the velocity potential into the boundary conditions (35) and (36), we have

$$\bar{\mathcal{L}}_1[\phi_1] = R_{1,1}(\xi_1, \xi_2) = \sum_{i=1}^{3}\sum_{j=-3}^{3} B_{1,1}^{i,j} \sin(i\,\xi_1 + j\,\xi_2), \tag{46}$$

$$\bar{\mathcal{L}}_2[\phi_1] = R_{1,2}(\xi_1, \xi_2) = \sum_{i=1}^{3}\sum_{j=-3}^{3} B_{1,2}^{i,j} \sin(i\,\xi_1 + j\,\xi_2), \tag{47}$$

respectively, where $B_{1,1}^{i,j}$ and $B_{1,2}^{i,j}$ are constants independent of ξ_1 and ξ_2. Note that these coefficients contain the two unknown constants $A_0^{1,0}$ and $A_0^{1,-1}$.

Since the auxiliary linear operator $\bar{\mathcal{L}}_2$ has the property

$$\bar{\mathcal{L}}_2[\Psi_{m,n}] = 0, \qquad \bar{\mathcal{L}}_2[F_{m,n}] = \sin(m\xi_1 + n\xi_2), \tag{48}$$

the general solution of (47) reads

$$\phi_1(\xi_1, \xi_2, z) = \sum_{i=1}^{3}\sum_{j=-3}^{3} \left(B_{1,2}^{i,j} F_{i,j} + A_1^{i,j} \Psi_{i,j} \right), \tag{49}$$

where $A_1^{i,j}$ are to-be-determined constants. Note that the above expression automatically satisfies the governing equation (34). Using the property (39) and substituting the above general solution into the boundary condition (46) gives us

$$\sum_{i=1}^{3}\sum_{j=-3}^{3} \lambda_{i,j} A_1^{i,j} \sin(i\xi_1 + j\xi_2)$$
$$= \sum_{i=1}^{3}\sum_{j=-3}^{3} \left[B_{1,1}^{i,j} - \frac{B_{1,2}^{i,j}}{\tanh\epsilon_1 \cosh(p\epsilon_1)} \right] \sin(i\,\xi_1 + j\,\xi_2). \tag{50}$$

According to (41) and (42), we have $\lambda_{1,0} = 0$ and $\lambda_{1,-1} = 0$ for the class-I Bragg resonance. Therefore, we must enforce

$$B_{1,1}^{1,0} - \frac{B_{1,2}^{1,0}}{\tanh\epsilon_1 \cosh(p\epsilon_1)} = 0, \qquad B_{1,1}^{1,-1} - \frac{B_{1,2}^{1,-1}}{\tanh\epsilon_1 \cosh(p\epsilon_1)} = 0$$

to avoid the so-called secular term, corresponding to the "singularity" occurred in perturbation approaches [31]. Since $B_{1,1}^{i,j}$ and $B_{1,2}^{i,j}$ contain the two unknown constants $A_0^{1,0}$ and $A_0^{1,-1}$, we gain the two coupled nonlinear algebraic equations

$$0.00059973 A_0^{1,0} - 6.04225 \left(A_0^{1,0} \right)^3 - 0.0000230462 A_0^{1,-1}$$
$$- 13.3757 A_0^{1,0} \left(A_0^{1,-1} \right)^2 = 0, \tag{51}$$

$$-0.0000230462 A_0^{1,0} + 0.00059973 A_0^{1,-1}$$
$$- 13.3757 \left(A_0^{1,0} \right)^2 A_0^{1,-1} - 6.04225 \left(A_0^{1,-1} \right)^3 = 0 \tag{52}$$

which have four groups of nontrivial solutions of $A_0^{1,0}$ and $A_0^{1,-1}$, as listed in Table 1. These multiple solutions result from the nonlinear terms of the surface boundary condition (14). All solutions with the same values of $\left| A_0^{1,0} \right|$ and $\left| A_0^{1,-1} \right|$ are in the same group, since they correspond to the same time-independent spectrum of wave energy, because the wave energy spectrum is determined by the amplitude square of wave components. For the sake of simplicity, only one solution of $A_0^{1,0}$ and $A_0^{1,-1}$ for each group is listed in Table 1. Note that each group in Table 1 corresponds to a different resonant wave, as shown later. It is well-known that nonlinear algebraic equations have multiple solutions. This is the mathematical reason why there exist the multiple equilibrium-state class-I Bragg resonant waves.

As long as $A_0^{1,0}$ and $A_0^{1,-1}$ are known, namely that the initial guess ϕ_0 is fixed, then $\eta_1(\xi_1, \xi_2)$ is obtained by (38), and in addition, all other constants $B_{1,1}^{i,j}$ in (46) and $B_{1,2}^{i,j}$ in (47) are determined. Further, equating the coefficients of Eq. (50), we have

$$A_1^{i,j} = \frac{1}{\lambda_{i,j}} \left[B_{1,1}^{i,j} - \frac{B_{1,2}^{i,j}}{\tanh\epsilon_1 \cosh(p\epsilon_1)} \right], \qquad \lambda_{i,j} \neq 0. \tag{53}$$

Since $\lambda_{1,0} = 0$ and $\lambda_{1,-1} = 0$, Eq. (50) holds for arbitrary $A_1^{1,0}$ and $A_1^{1,-1}$. In other words, they cannot be determined by the above expression. Therefore, like the initial guess $\phi_0(\xi, \xi_2, z)$ defined by (43), the solution $\phi_1(\xi_1, \xi_2, z)$ still contains two unknown parameters $A_1^{1,0}$ and $A_1^{1,-1}$, which can be determined in a similar way by avoiding the so-called secular term of $\phi_2(\xi_1, \xi_2, z)$.

Table 1
Solutions of the nonlinear algebraic equations (51) and (52) when the resonant condition (2) is satisfied in the case of (44).

$A_0^{1,0}$	$A_0^{1,-1}$
Group 1	
−0.00995774	0.000315596
0.00995774	−0.000315596
Group 2	
−0.00566324	0.00566324
0.00566324	−0.00566324
Group 3	
−0.00544964	−0.00544964
0.00544964	0.00544964
Group 4	
−0.000315596	0.00995774
0.000315596	−0.00995774

In this way, we can successively gain $\eta_2(\xi_1, \xi_2)$, $\phi_2(\xi_1, \xi_2, z)$, $\eta_3(\xi_1, \xi_2)$, $\phi_3(\xi_1, \xi_2, z)$, and so on. Note that the high-order deformation equations are linear, and only fundamental operations are needed in the above HAM-based approach. Thus, using the computer algebra software (such as Mathematica), we can obtain the approximations of the velocity potential $\phi(\xi_1, \xi_2, z)$ and the wave elevation $\eta(\xi_1, \xi_2)$ efficiently.

It should be emphasized that the velocity potential $\phi(\xi_1, \xi_2, z)$ and wave elevation $\eta(\xi_1, \xi_2)$ contain the so-called "convergence-control parameter" c_0, whose value is unknown up to now. This is mainly because, in the frame of the HAM, one can introduce the "convergence-control parameter", which has no physical meanings. However, as illustrated by Liao [7–11], the convergence-control parameter c_0 provides a simple way to guarantee the convergence of analytic approximations. A proper value of the convergence-control parameter c_0 is determined when the averaged squared residuals of the governing equations decrease fast. The averaged squared residuals of the governing equations (23)–(25) are defined as follows:

$$\varepsilon_{m,1} = \frac{1}{(1+M)^2} \sum_{i=0}^{M} \sum_{j=0}^{M} \left[\sum_{n=0}^{m} \Delta_n^\phi(i\Delta\xi_1, j\Delta\xi_2) \right]^2, \tag{54}$$

$$\varepsilon_{m,2} = \frac{1}{(1+M)^2} \sum_{i=0}^{M} \sum_{j=0}^{M} \left[\sum_{n=0}^{m} \Delta_n^\eta(i\Delta\xi_1, j\Delta\xi_2) \right]^2, \tag{55}$$

$$\varepsilon_{m,3} = \frac{1}{(1+M)^2} \sum_{i=0}^{M} \sum_{j=0}^{M} \left[\sum_{n=0}^{m} \Delta_n^b(i\Delta\xi_1, j\Delta\xi_2) \right]^2, \tag{56}$$

respectively, where M is the discrete number and $\Delta\xi_1 = \Delta\xi_2 = \pi/M$. In this article, we use $M = 10$.

The residuals should tend to zero as the approximation order increases if this convergence-control parameter c_0 is properly chosen. Since the governing equation (22) is automatically satisfied, it is our main task to choose a proper c_0 in order to make sure that the averaged squared residuals of the boundary conditions (23)–(25) decrease as the order of approximations increase.

For instance, let us consider Group 1 in Table 1, with $A_0^{1,0} = -0.00995774$ and $A_0^{1,-1} = 0.000315596$. The corresponding averaged residual squares $\varepsilon_{m,i}$ ($i = 1, 2, 3$) at different order m of approximations are shown in Fig. 4. It is found that, as the order of approximation increases, the averaged residual squares of the three boundary conditions decrease in an interval around $c_0 \in [-1, 7, -0.5]$ with a fast decrease near $c_0 = -1.2$. So, we choose $c_0 = -1.2$ as an optimal convergence-control parameter. As long as c_0 is determined, the mth-order approximations of the velocity potential $\phi(\xi_1, \xi_2, z)$ and wave elevation $\eta(\xi_1, \xi_2)$ are completely
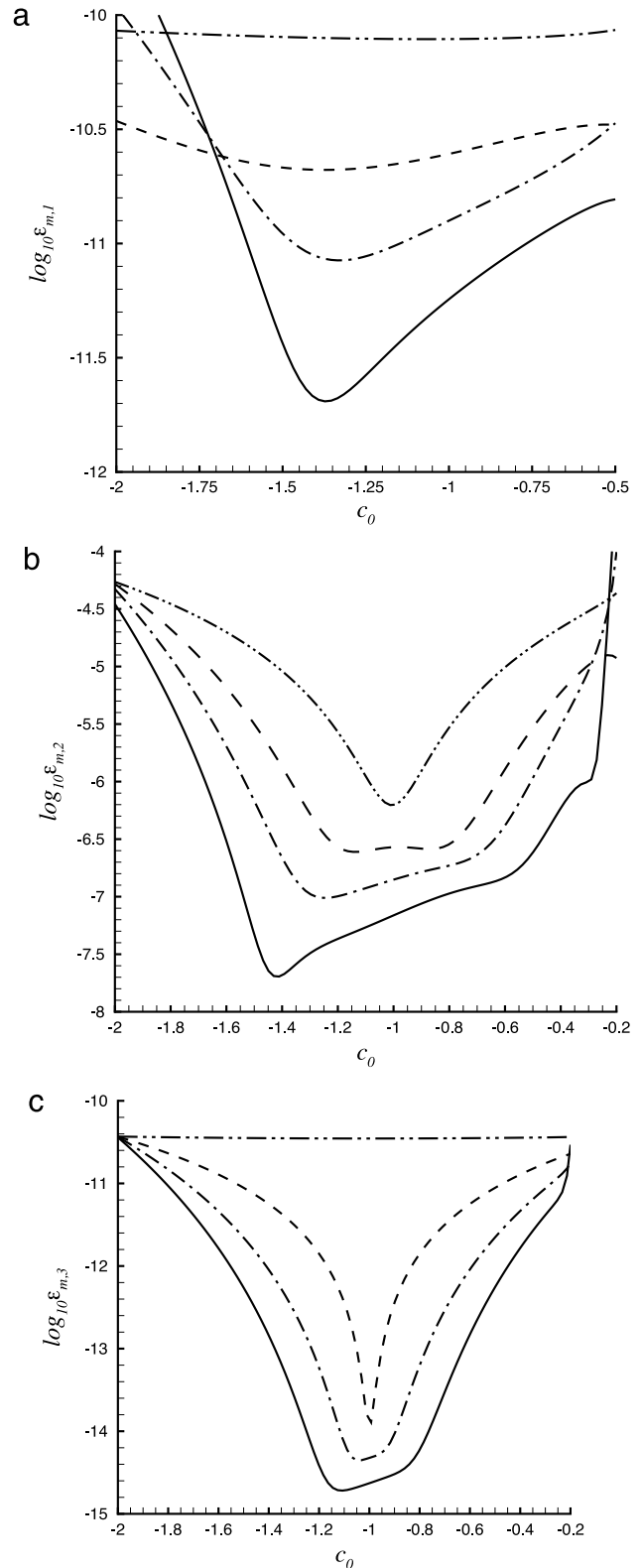
Fig. 4. Averaged residual squares versus c_0 in the case of $\alpha = 70°$, $k_B/k = 0.68404$, $kd = 2.5$, $bk_B = 0.005$, $\epsilon = 1.0003$ when $A_0^{1,0} = -0.00995774$ and $A_0^{1,-1} = 0.000315596$ (corresponding to Group 1). Dash-dot-dotted line: 1st-order approximation; Dashed line: 2nd-order approximation; Dash-dotted line: 3rd-order approximation; Solid line: 4th-order approximation.

known. Fig. 5 summarizes the averaged residual squares of the three boundary conditions at different order of approximations when $c_0 = -1.2$. All of them decrease as the order m increases,
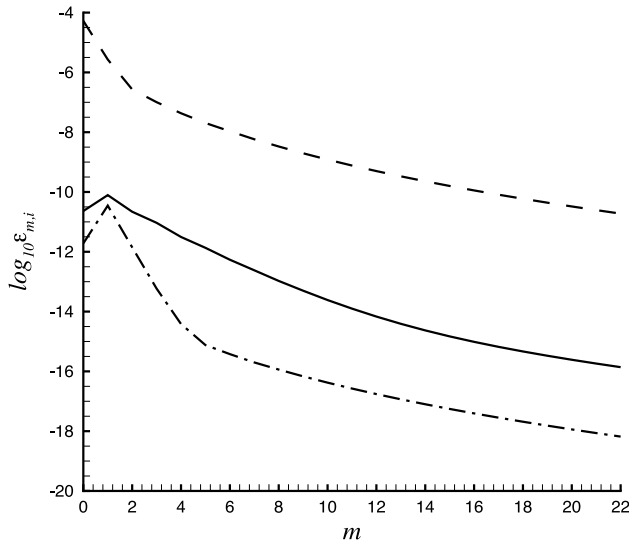
Fig. 5. Averaged residual squares versus the approximation order m by means of $c_0 = -1.2$ in the case of $\alpha = 70°$, $k_B/k = 0.68404$, $kd = 2.5$, $bk_B = 0.005$, $\epsilon = 1.0003$ when $A_0^{1,0} = -0.00995774$ and $A_0^{1,-1} = 0.000315596$ (corresponding to Group 1). Solid line: $\log_{10} \varepsilon_{m,1}$; Dashed line: $\log_{10} \varepsilon_{m,2}$; Dash-dotted line: $\log_{10} \varepsilon_{m,3}$.

Table 2
Wave energy distribution for different equilibrium states of the class-I Bragg resonant wave system in the case of $\alpha = 70°$, $k_B/k = 0.68404$, $kd = 2.5$, $bk_B = 0.005$ and $\epsilon = 1.0003$.

	Distribution of wave energy		
	Wave A $a_{1,0}^2/\Pi$	Wave C $a_{1,-1}^2/\Pi$	Sum Π_0/Π
Group 1	0.8620	0.1378	0.9998
Group 2	0.4999	0.4999	0.9998
Group 3	0.4999	0.4999	0.9998
Group 4	0.1378	0.8620	0.9998

indicating the convergence of our analytic approximations of the class-I Bragg resonant waves, corresponding to Group 1 in Table 1. Thus, using the initial approximation of Group 1 listed in Table 1, we gain an equilibrium-state class-I Bragg resonant wave.

Similarly, we can gain the different equilibrium-state class-I Bragg resonant waves by means of the initial guesses of Group 2 to 4 listed in Table 1. The corresponding wave energy distributions are listed in Table 2, where

$$\Pi = \sum_{i=0}^{+\infty} \sum_{j=-\infty}^{+\infty} a_{i,j}^2 \qquad (57)$$

is directly proportional to the total wave energy, and

$$\Pi_0 = a_{1,0}^2 + a_{1,-1}^2 \qquad (58)$$

the sum of wave energy for the wave components A and C only, respectively. Thus, $a_{1,0}^2/\Pi$ and $a_{1,-1}^2/\Pi$ denote the ratio of wave energy of the wave A and wave C to the total wave energy, respectively.

As shown in Table 2, the equilibrium-state class-I Bragg resonant waves of Group 1 and Group 4 have the anti-symmetric wave energy distribution between the wave A and wave C. So do the solutions of Group 2 and Group 3. This is because the two wave components with wavenumbers $\boldsymbol{k}_A$ and $\boldsymbol{k}_C$ are symmetric on the perpendicular bisector of the bottom wavenumber $\boldsymbol{k}_B$, as shown in Fig. 2. Since the shape of bottom are fixed, both of $\boldsymbol{k}_B$ and $-\boldsymbol{k}_B$ can be regarded as the wavenumber of the bottom ripples. So, either wave A or wave C can be regarded as the resonant wave. Opposite bottom wavenumber $-\boldsymbol{k}_B$ makes $\boldsymbol{k}_C$ to be the wavenumber of the primary

wave and $\boldsymbol{k}_A$ the resonant ones, respectively. So, it is not important to define which wave component corresponds to the primary wave and which to the resonant ones. If anyone among $\boldsymbol{k}_A$ and $\boldsymbol{k}_C$ is regarded as the wavenumber of the primary wave, the other is for the resonant one. Thus, due to the antisymmetry, only two different kinds of equilibrium-state class-I Bragg resonant waves are found. For the first kind of equilibrium-state resonant wave system (corresponding to Group 2 and 3 in Table 2), the amplitude of the wave A is equal to that of the wave C, so that the primary and resonant wave components contain the same wave energy. This kind of class-I Bragg resonant waves is similar to the first-order multiple-scale approximation given by Mei [25] in the limiting case of the infinite ripples, as discussed later. However, for the second kind (corresponding to Group 1 and 4 in Table 2), the wave A and wave C contain different wave energy. This kind of equilibrium-state class-I Bragg resonant waves have never been reported, to the best of our knowledge. Note that these two kinds of equilibrium-state class-I Bragg resonant waves widely exist in general cases, as shown below.

5. Bifurcations of equilibrium-state resonant waves

The HAM-based analytic approach described in Section 4 is valid in general for different physical parameters $\epsilon_1 = kd$, $\epsilon_2 = bk_B$, $\epsilon_3 = k_B/k = 2\cos\alpha$ and ϵ. In this section, we investigate the effect of the wave propagation angle α of the wave A (with wavenumber $\boldsymbol{k}_A$), the bottom slope (denoted by $\epsilon_2 = bk_B$), the water depth (denoted by $\epsilon_1 = kd$) and the nonlinearity (ϵ) on the equilibrium states of the class-I Bragg resonant waves. As shown below, two kinds of equilibrium-state class-I Bragg resonant waves are found with a bifurcation, and one among them has been never reported.

5.1. Equilibrium-state resonant waves for different wave propagation angle α

Let us first consider the effect of the propagation angle α of the wave A with the wavenumber $\boldsymbol{k}_A$ on the equilibrium states of the class-I Bragg resonant waves. Without loss of generality, consider the following case

$$\epsilon_1 = kd = 2.5, \qquad \epsilon_2 = bk_B = 0.005, \qquad \epsilon = 1.0003 \qquad (59)$$

with various propagation angle α of the wave A. In a similar way as mentioned in Section 4, two kinds of equilibrium states of class-I Bragg resonant waves are found. The wave A and wave C share the same wave energy for the 1st kind of equilibrium-state ($a_{1,0}^2/\Pi = a_{1,-1}^2/\Pi = 0.499$) for different angles in the domain $0 < \alpha < 75(°)$. The corresponding wave energy distributions for the 2nd kind of equilibrium-state is shown in Table 3. Both of the two equilibrium states are depicted by Fig. 6.

Our results indicate that there exist two kinds of equilibrium-state class-I Bragg resonant waves, with a bifurcation with respect to the propagation angle α of the wave A. For the first kind, the wave components A and C contain the same wave energy ($a_{1,0}^2/\Pi = a_{1,-1}^2/\Pi = 0.499$). This agrees well with the multiple-scale approximation given by Mei [25] for the perfect tuning ($\Omega = 0$) resulting from the linearized governing equations. For the second kind, they have different wave energy, as listed in Table 3. Note that, from physical viewpoint, there should be no resonant waves when the propagation angle α tends to 90°. Thus, the first kind of equilibrium-state class-I Bragg resonant waves should have no physical meanings for large α close to 90°. From physical viewpoint, as α decreases from 90° to zero, the resonant wave should appear with more and more wave energy, i.e. higher and higher wave amplitude. This is indeed true. For the second kind of equilibrium-state class-I Bragg resonant waves, the primary

Table 3
Wave energy distribution of the 2nd kind of equilibrium state of the class-I Bragg resonant wave system with different propagation angle α of the wave A in the case of $kd = 2.5$, $bk_B = 0.005$ and $\epsilon = 1.0003$.

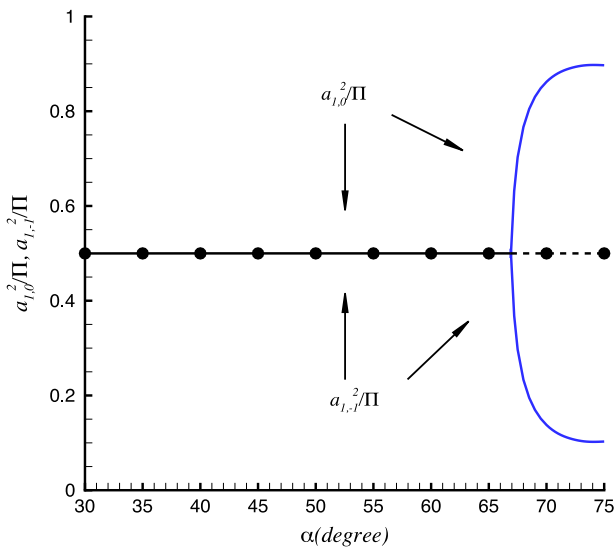| α (deg)	Distribution of wave energy		
	Wave A (C) $a_{1,0}^2/\Pi$	Wave C (A) $a_{1,-1}^2/\Pi$	Sum Π_0/Π
66.9	0.48998	0.50988	0.99986
67	0.5384	0.4615	0.9999
67.2	0.6317	0.3682	0.9999
67.5	0.7029	0.2970	0.9999
68	0.7667	0.2332	0.9999
68.5	0.8047	0.1952	0.9999
69	0.8303	0.1696	0.9999
69.5	0.8485	0.1513	0.9998
70	0.8620	0.1378	0.9998
72	0.8903	0.1096	0.9999
73.5	0.8972	0.1026	0.9998
75	0.8970	0.1028	0.9998

Fig. 6. Wave energy distribution versus propagation angle α for the equilibrium states of the class-I Bragg resonant wave system in the case of $kd = 2.5$, $bk_B = 0.005$ and $\epsilon = 1.0003$.

wave contains almost all wave energy for large α close to 90°, and then, as α decreases, it has less and less wave energy until $\alpha \approx 66.9°$. In other words, as α decreases from 90° to 66.9°, the resonant wave has more and more wave energy. A bifurcation of solutions occurs at $\alpha \approx 66.9°$, as shown in Fig. 6. Thus, the second kind of equilibrium-state class-I Bragg resonant waves is physically more reasonable for large propagation angle α of the wave A. So, such kind of bifurcation of equilibrium-state class-I Bragg resonant waves with respect to the propagation angle α of the wave A is physically reasonable. It should be emphasized that the second kind of equilibrium-state class-I Bragg resonant waves and especially the bifurcation with respect to α have never been reported.

It is well-known that bifurcation is a common characteristic of nonlinear dynamic systems. Obviously, such kind of bifurcation cannot be found by means of linearized wave theory. This indicates the importance of the nonlinearity for the class-I Bragg resonant waves.

5.2. Equilibrium-state resonant waves for different water depth kd

Secondly, let us study the effect of the dimensionless water depth kd on the equilibrium states of class-I Bragg resonant waves.
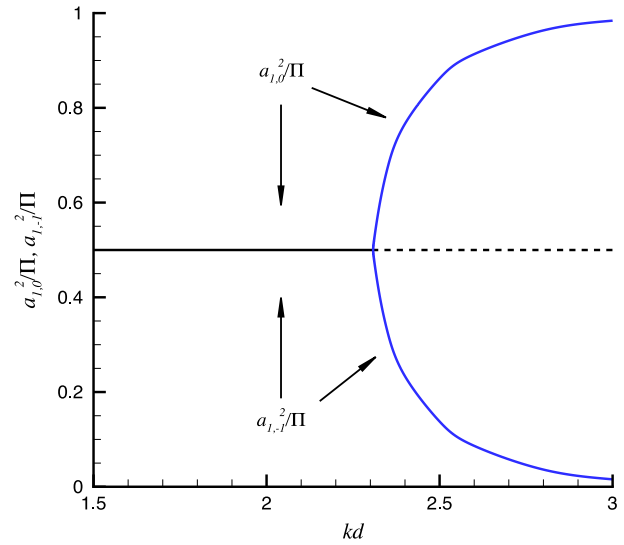

Fig. 7. Wave energy distribution versus kd of the equilibrium states of the class-I Bragg resonant wave system in the case of $\alpha = 70°$, $k_B/k = 0.68404$, $bk_B = 0.005$ and $\epsilon = 1.0003$.

Table 4
Wave energy distribution of the 2nd kind of equilibrium state of the class-I Bragg resonant wave system at different water depth (kd) in the case of $\alpha = 70°$, $k_B/k = 0.68404$, $bk_B = 0.005$ and $\epsilon = 1.0003$.

kd	Distribution of wave energy		
	Wave A (C) $a_{1,0}^2/\Pi$	Wave C (A) $a_{1,-1}^2/\Pi$	Sum Π_0/Π
2.31	0.5170	0.4829	0.9999
2.325	0.5891	0.4107	0.9998
2.35	0.6743	0.3256	0.9999
2.4	0.7664	0.2334	0.9998
2.5	0.8620	0.1378	0.9998
2.6	0.9134	0.0864	0.9998
2.8	0.9635	0.0363	0.9998
3	0.9841	0.0157	0.9998

Without loss of generality, consider the following case

$$\alpha = 70°, \qquad \epsilon_2 = bk_B = 0.005,$$

$$\epsilon_3 = \frac{k_B}{k} = 0.68404, \qquad \epsilon = 1.0003 \tag{60}$$

with various dimensionless water depth $\epsilon_1 = kd$.

In a similar way as described in Section 4, two kinds of equilibrium-state class-I Bragg resonant waves are found with a bifurcation with respect to the dimensionless water depth kd, as shown in Fig. 7. For the first kind, the primary and resonant waves have the same wave energy, i.e. $a_{1,0}^2/\Pi = a_{1,-1}^2/\Pi = 0.499$ for different mean water depth in the domain $1.5 < kd < 3$. For the second kind, they contain different wave energy, as shown in Table 4. Note that, physically speaking, for deep water, i.e. as $kd \to +\infty$, there should be no resonant wave caused by the bottom ripples. So, the first kind of equilibrium-state resonant waves might have no physical meanings in deep water, say, as $kd \to +\infty$. However, as the water depth becomes smaller and smaller, the influence of bottom ripples becomes more and more important, so that the resonant wave component should contain more and more wave energy, until both of the primary wave and resonant wave have the same wave amplitude. This is indeed true, as shown in Fig. 7 which clearly indicates the bifurcation at $kd \approx 2.3$. So, such kind of bifurcation with respect to the dimensionless water depth kd is reasonable from the physical viewpoint.

It should be emphasized that the two kinds of equilibrium-state class-I Bragg resonant waves and especially the bifurcation
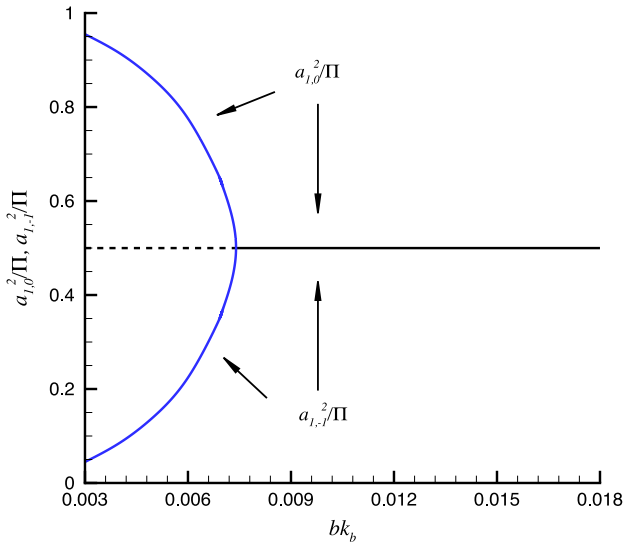
Fig. 8. Wave energy distribution versus the bottom slope bk_B of the equilibrium states of the class-I Bragg resonant wave system in the case of $\alpha = 70°$, $k_B/k = 0.68404$, $kd = 2.5$ and $\epsilon = 1.0003$.

with respect to the water depth kd have never been reported, to the best of our knowledge. Note that bifurcation is a common characteristic of nonlinear dynamic system. This indicates once again the important influence of nonlinearity of the class-I Bragg resonant waves.

5.3. Equilibrium-state resonant waves for different bottom slope bk_B

Let us study the effect of the bottom slope bk_B on the equilibrium-state class-I Bragg resonant waves. Without loss of generality, consider the case

$$\alpha = 70°, \qquad \epsilon_1 = kd = 2.5,$$
$$\epsilon_3 = k_B/k = 0.68404, \qquad \epsilon = 1.0003, \tag{61}$$

with various bottom slope $\epsilon_2 = b\,k_B$.

In a similar way as described in Section 4, two kinds of equilibrium states of class-I Bragg resonant waves with a bifurcation with respect to the bottom slope bk_B are found as well, as shown in Fig. 8. For the first kind, the primary wave and the resonant ones have the same wave energy, i.e. $a_{1,0}^2/\Pi = a_{1,-1}^2/\Pi = 0.499$ for different bottom slope in the domain $0.003 < bk_B < 0.018$. For the second kind, they have different wave energy, as shown in Table 5. However, from physical viewpoint, as the bottom slope $bk_B \to 0$, i.e. the bottom is flat, there should be no resonance caused by the bottom ripples, say, the class-I Brag resonance should not exist at all. Thus, the first kind of equilibrium-state class-I Bragg resonant waves should have no physical meanings for the flat bottom, say, as $bk_B \to 0$. From physical viewpoint, as the bottom slope bk_B becomes larger and larger, the resonant wave should contain more and more wave energy, until both of the primary and resonant waves have the same wave amplitude. This is indeed true, as shown in Fig. 8, which clearly indicates the bifurcation with respect to the bottom slope at $bk_B \approx 0.0074$. So, such kind of bifurcation with respect to the bottom slope is reasonable from the physical viewpoint.

It should be emphasized that the two kinds of equilibrium-state class-I Bragg resonant waves and especially the bifurcation with respect to the bottom slope bk_B have never been reported, to the best of our knowledge. Note that bifurcation is a common characteristic of nonlinear dynamic system. This indicates once again the important influence of nonlinearity of the class-I Bragg resonant waves.

Table 5
Wave energy distribution of the 2nd kind of equilibrium state of the class-I Bragg resonant wave system with different bottom slope (bk_B) in the case of $\alpha = 70°$, $k_B/k = 0.68404$, $kd = 2.5$ and $\epsilon = 1.0003$.

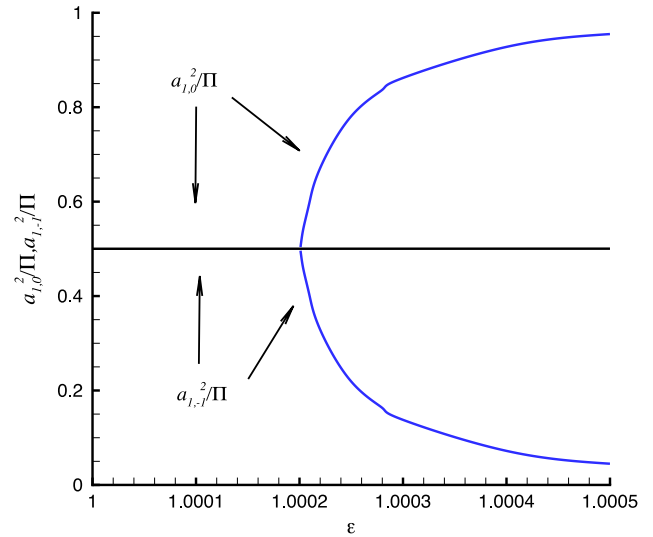| bk_B	Distribution of wave energy		
	Wave A (C) $a_{1,0}^2/\Pi$	Wave C (A) $a_{1,-1}^2/\Pi$	Sum Π_0/Π
0.003	0.9550	0.0448	0.9998
0.004	0.9169	0.0830	0.9999
0.005	0.8620	0.1378	0.9998
0.006	0.7820	0.2178	0.9998
0.007	0.6345	0.3653	0.9998
0.00725	0.5653	0.4346	0.9999
0.0074	0.5004	0.4994	0.9998

Fig. 9. Wave energy distribution versus the nonlinearity ϵ of the equilibrium states of the class-I Bragg resonant wave system in the case of $\alpha = 70°$, $k_B/k = 0.68404$, $kd = 2.5$ and $bk_B = 0.005$.

5.4. Equilibrium-state resonant waves for different nonlinearities ϵ

Finally, let us study the effect of the nonlinearity ϵ on the equilibrium-state class-I Bragg resonant waves. Without loss of generality, consider the case

$$\alpha = 70°, \qquad kd = 2.5, \qquad k_B/k = 0.68404,$$
$$bk_B = 0.005. \tag{62}$$

In a similar way, two kinds of equilibrium states of class-I Bragg resonant waves with a bifurcation with respect to the nonlinearity ϵ are found as well, as shown in Fig. 9. For the first kind, the primary wave and the resonant one have the same wave energy, i.e. $a_{1,0}^2/\Pi = a_{1,-1}^2/\Pi = 0.499$ for different nonlinearities in the domain $1.00008 < \epsilon < 1.0005$. For the second kind, they have different wave energy, as shown in Table 6. From physical viewpoint, the bifurcation is due to nonlinearity. As presented by Fig. 9, when the nonlinearity ϵ increases, the bifurcation appears at $\epsilon \approx 1.0002$. When ϵ grows further, the resonant wave contains more and more wave energy in the second kind of equilibrium state. In addition, the bifurcation points shift as the nonlinearity ϵ varies. Take the bifurcation point of the incident angle α as an example. Let us investigate the case

$$kd = 2.5, \qquad k_B/k = 0.68404, \qquad bk_B = 0.005. \tag{63}$$

For each ϵ, there should be a corresponding bifurcation point α_{bif}. When ϵ increases from 1.0001 to 1.0003, the bifurcation point of α_{bif} decreases from 79.5° to 66.9°, as shown by Fig. 10. This means the bifurcation will start earlier for larger nonlinearity which varies

Table 6

Wave energy distribution of the 2nd kind of equilibrium state of the class-I Bragg resonant wave system with different nonlinearity (ϵ) in the case of $\alpha = 70°$, $k_B/k = 0.68404$, $kd = 2.5$ and $bk_B = 0.005$.

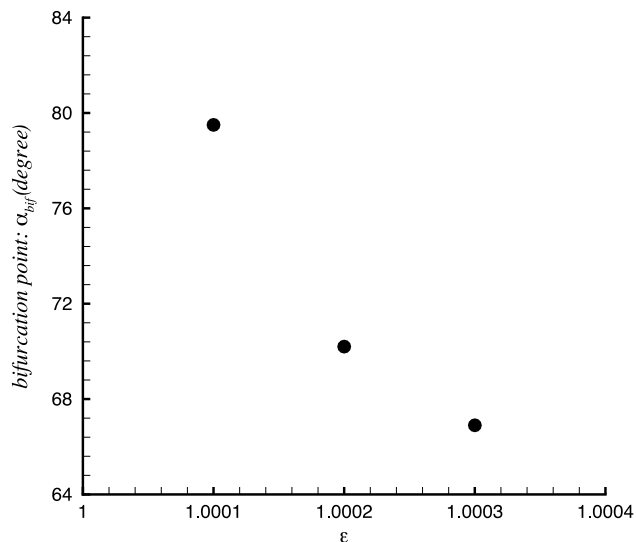| ϵ	Distribution of wave energy		
	Wave A (C) $a_{1,0}^2/\Pi$	Wave C (A) $a_{1,-1}^2/\Pi$	Sum Π_0/Π
1.000201	0.5038	0.4961	0.9999
1.000205	0.5559	0.4440	0.9999
1.00021	0.6024	0.3975	0.9999
1.00022	0.6709	0.3290	0.9999
1.00025	0.7809	0.2190	0.9999
1.00028	0.8369	0.1630	0.9999
1.0003	0.8620	0.1378	0.9998
1.0004	0.9277	0.0721	0.9998
1.0005	0.9549	0.0449	0.9999

Fig. 10. Bifurcation points of the incident angle versus the nonlinearity ϵ of the equilibrium states of the class-I Bragg resonant wave system in the case of $k_B/k = 0.68404$, $kd = 2.5$ and $bk_B = 0.005$.

in the domain of $\alpha_{bif} \in (1.0001, 1.0003)$ if the incident angle starts from zero. Thus, stronger nonlinearity makes bifurcation easier.

5.5. Physical analysis of the two equilibrium states

From the physical viewpoint, the resonant wave should have less and less wave energy as the effects of Bragg resonance decrease, which correspond to the cases when the water depth becomes deep, the slope of bottom ripples decreases, and the wave direction becomes increasingly parallel to the ripples. It should be emphasized that the 2nd kind of equilibrium-state is physically more reasonable for the case with less effects of Bragg resonance. As the effects of Bragg resonance increase, the resonant wave has more and more wave energy until the bifurcations. After the bifurcations, it shares the same energy with the primary wave corresponding to the 1st equilibrium state, as depicted by Figs. 6–8.

6. Concluding remarks and discussions

For the class-I Bragg resonant wave systems about the nonlinear interaction between surface waves and bottom ripples, Mitra and Greenberg [30] found the slowly periodic exchange of wave energy between different wave modes, say, the wave amplitude and frequency of each component changes periodically with the time. They solved the problem from the viewpoint of initial value equations, and thus did not gain any multiple resonant waves,

since an initial value problem has only one solution. Their work agreed with the famous conclusion of Benney [2] for periodically varying surface resonant waves. Davies [31] applied perturbation method to search for equilibrium states of the class-I Bragg resonant waves, but failed, mainly because "the perturbation theory breaks down due to singularities in the transfer functions", as currently also pointed out by Madsen and Fuhrman [6]. It was an open question whether or not there exist the equilibrium-states of the class-I Bragg resonant waves, whose amplitude and frequency of each components are independent of time.

In this paper, using an advanced analytic approximation method for nonlinear problems, namely the homotopy analysis method (HAM) [7–13], we successfully obtain the two kinds of the equilibrium-states of the class-I Bragg resonant wave systems with bifurcations. For the first kind, the primary and resonant wave components have the same amplitude, i.e. the same wave energy. This agrees well with the perfect tuning case ($\Omega = 0$) reported by Mei [25] using a linearized wave equation. However, for the second kind, they contain different wave energy, which have been never reported. Especially, the bifurcations of the equilibrium-state solutions with respect to the wave propagation angle α of the primary wave, the dimensionless water depth kd, the bottom slope bk_B and the nonlinearity ϵ, as shown in Figs. 6–9, respectively, were discovered for the first time. As mentioned in Section 5, these bifurcations are reasonable from physical viewpoints. Note that bifurcation is a common characteristic of nonlinear dynamic systems. It should be emphasized that the second kind of equilibrium-state class-I Bragg resonant waves and especially the bifurcations have been never reported, to the best of our knowledge. This also indicates the importance of the nonlinearity for the class-I Bragg resonant waves. All of these reveal the novel of our work.

Mathematically, unlike previous approaches, we use the homotopy analysis method (HAM) [7–13], an advanced analytic approximation method for nonlinear problems. Unlike perturbation methods, the HAM is independent of small/large physical parameters. So, it is unnecessary for us to assume any small physical parameters in our HAM-based approach. It allows one to solve a target nonlinear problem via a perturbation expansion about a parameter that is not physical (called embedding parameter). The embedding parameter allows one to interpolate between a suitably chosen linear problem (with known solution) and the target nonlinear problem (with unknown solution). The method provides a series solution for the target nonlinear problem which converges if the solution of the linear problem and the solution of the target problem are homotopic. Since we do not know a priori the homotopy class of the solution of the target nonlinear problem, it follows that the choice of the linear problem is very important. In particular, the convergence of the HAM method will depend crucially on this choice. In addition, *provided the original nonlinear problem is homotopic to the associated linear sub-problems*, the HAM provides us a simple way (convergent-control parameter c_0) to greatly improve the convergence speed of the solution series. Especially, unlike previous approaches which regarded the class-I Bragg resonance as an initial value problem that leads to slowly periodic solutions, we search for the equilibrium states of the resonant waves, which are unknown and governed by a nonlinear boundary-value problem. It is well-known that nonlinear boundary-value problems often have multiple solutions. This is the mathematical reason why we gain the two different types of the equilibrium-state class-I Bragg resonant waves with the bifurcations.

Combining our equilibrium-state resonant waves with the periodic resonant ones given by Mitra and Greenberg [30], we have now a better understanding about the class-I Bragg resonance. From the traditional viewpoint of initial-value problems, the class-I Bragg resonant wave systems have periodically varying

amplitudes and frequencies of wave components if the initial condition is randomly given, but are time-independent if the initial condition is given exactly according to the equilibrium-states of the class-I Bragg resonant ones found in this paper. Note that the class-I Bragg resonant wave is a complicated nonlinear dynamic system, and these equilibrium-states and especially their bifurcations discovered in this article reveal one of its important, global property of nonlinear dynamics. So, this work is helpful to deepen and enrich our understandings about the class-I Brag resonance.

It should be mentioned that for cases with large incidence angle, large water depth and small bottom slope, the equilibrium state is unreasonable where the two wave components have the same wave energy. This state is possibly unstable physically while the two kinds equilibrium states for relatively large nonlinearity are not unreasonable apparently. Thus the stability of the equilibrium states will be considered in the future. In addition, for simplicity, an infinite number of ripples on the bottom is considered approximately when the ripples are located in a large area. The result found in this paper might be extended into the optics which can propagate for quite long distance, where the Bragg resonance were found initially of the X-ray diffraction by William Lawrence Bragg and William Henry Bragg [33], who were awarded the Nobel Prize in Physics in 1915.

Can we observe the two kinds of the equilibrium-states of the class-I Bragg resonant waves with the bifurcations in laboratory? Are they stable? How about the class-II and class-III Bragg resonant wave systems? Obviously, further theoretical, numerical and experimental studies are necessary in future to answer these interesting open questions.

Acknowledgments

Appendix. Detailed mathematical deduction of the high-order deformation equations (35)–(38)

The HAM is based on the homotopy, a basic concept of topology, which may describe continuous variations (or deformations) of functions. In the context of the HAM, we first construct the continuous variations $\check{\phi}(\xi_1, \xi_2, z; q)$ and $\check{\eta}(\xi_1, \xi_2; q)$ which, as the embedding parameter $q \in [0, 1]$ increases from 0 to 1, continuously deform from the initial guesses $\phi_0(\xi_1, \xi_2, z)$ and $\eta_0(\xi_1, \xi_2)$ to the solution $\phi(\xi_1, \xi_2, z)$ and $\eta(\xi_1, \xi_2)$ of the boundary-value Eqs. (22)–(25), respectively.

Such continuous variations are governed by the zeroth-order deformation equation

$$\left(\frac{\partial^2}{\partial \xi_1^2} + 2\epsilon_3 \cos\alpha \frac{\partial^2}{\partial \xi_1 \partial \xi_2} + \epsilon_3^2 \frac{\partial^2}{\partial \xi_2^2} + \frac{\partial^2}{\partial z^2} \right)$$
$$\times \check{\phi}(\xi_1, \xi_2, z; q) = 0 \tag{A.1}$$

in the domain $-\epsilon_1 + q(\epsilon_2/\epsilon_3)\cos(\xi_2) < z < \epsilon_1 \check{\eta}(\xi_1, \xi_2; q)$, subject to the boundary conditions on the unknown free surface $z = \epsilon_1 \check{\eta}(\xi_1, \xi_2; q)$,

$$(1-q)\mathcal{L}_1[\check{\phi}(\xi_1, \xi_2, z; q) - \phi_0(\xi_1, \xi_2, z)]$$
$$= q\, c_0\, \mathcal{N}_1[\check{\phi}(\xi_1, \xi_2, z; q)], \tag{A.2}$$

$$(1-q)\check{\eta}(\xi_1, \xi_2; q) = q\, c_0\, \mathcal{N}_2[\check{\phi}(\xi_1, \xi_2, z; q), \check{\eta}(\xi_1, \xi_2; q)], \tag{A.3}$$

and the bottom condition on $z = -\epsilon_1 + q(\epsilon_2/\epsilon_3)\cos\xi_2$,

$$(1-q)\mathcal{L}_2[\check{\phi}(\xi_1, \xi_2, z; q) - \phi_0(\xi_1, \xi_2, z)]$$
$$= q\, c_0\, \mathcal{N}_3[\check{\phi}(\xi_1, \xi_2, z; q)], \tag{A.4}$$

where $\mathcal{L}_i$ ($i = 1, 2$) are the auxiliary linear operators with the property $\mathcal{L}_i[0] = 0$, $c_0 \neq 0$ is the convergence-control parameter, and

$$\mathcal{L}_1 = \frac{\partial^2}{\partial \xi_1^2} + \frac{1}{\tanh(\epsilon_1)} \frac{\partial}{\partial z}, \qquad \mathcal{L}_2 = \frac{\partial}{\partial z}, \tag{A.5}$$

$$\mathcal{N}_1[\check{\phi}] = \frac{\partial^2 \check{\phi}}{\partial \xi_1^2} + \frac{1}{\epsilon^2 \tanh(\epsilon_1)} \frac{\partial \check{\phi}}{\partial z} - 2\epsilon_1 \frac{\partial \check{f}}{\partial \xi_1} + \epsilon_1^2 \nabla \check{\phi} \cdot \nabla \check{f}, \tag{A.6}$$

$$\mathcal{N}_2[\check{\phi}, \check{\eta}] = \check{\eta} - \epsilon^2 \tanh(\epsilon_1) \left(\frac{\partial \check{\phi}}{\partial \xi_1} - \epsilon_1 \check{f} \right), \tag{A.7}$$

$$\mathcal{N}_3[\check{\phi}] = \frac{\partial \check{\phi}}{\partial z} + \epsilon_2 \sin\xi_2 \left(\cos\alpha \frac{\partial \check{\phi}}{\partial \xi_1} + \epsilon_3 \frac{\partial \check{\phi}}{\partial \xi_2} \right), \tag{A.8}$$

$$\check{f}(\check{\phi}) = \frac{1}{2} \left[\left(\frac{\partial \check{\phi}}{\partial \xi_1} \right)^2 + \epsilon_3^2 \left(\frac{\partial \check{\phi}}{\partial \xi_2} \right)^2 \right.$$
$$\left. + 2\epsilon_3 \cos\alpha \frac{\partial \check{\phi}}{\partial \xi_1} \frac{\partial \check{\phi}}{\partial \xi_2} + \left(\frac{\partial \check{\phi}}{\partial z} \right)^2 \right], \tag{A.9}$$

respectively. The homotopy-series solutions of the velocity potential and wave elevation are

$$\phi(\xi_1, \xi_2, z) = \sum_{m=0}^{+\infty} \phi_m(\xi_1, \xi_2, z), \tag{A.10}$$

$$\eta(\xi_1, \xi_2) = \sum_{m=0}^{+\infty} \eta_m(\xi_1, \xi_2), \tag{A.11}$$

where

$$\phi_m(\xi_1, \xi_2, z) = \frac{1}{m!} \left. \frac{\partial^m \check{\phi}(\xi_1, \xi_2, z; q)}{\partial q^m} \right|_{q=0}, \tag{A.12}$$

$$\eta_m(\xi_1, \xi_2) = \frac{1}{m!} \left. \frac{\partial^m \check{\eta}(\xi_1, \xi_2; q)}{\partial q^m} \right|_{q=0}. \tag{A.13}$$

And further, the Mth-order homotopy approximation reads

$$\phi(\xi_1, \xi_2, z) \approx \sum_{m=0}^{M} \phi_m(\xi_1, \xi_2, z), \tag{A.14}$$

$$\eta(\xi_1, \xi_2) \approx \sum_{m=0}^{M} \eta_m(\xi_1, \xi_2), \tag{A.15}$$

where $\phi_m(\xi_1, \xi_2, z)$ and $\eta_m(\xi_1, \xi_2)$ are obtained by solving the high-order deformation equations derived as follows. Based on the

zeroth-order deformation Eqs. (A.1)–(A.4) and following Liao [14], we define

$$\mu_{1,n} = \eta_n, \quad n \geq 1, \tag{A.16}$$

$$\mu_{m,n} = \sum_{i=m-1}^{n-1} \mu_{m-1,i}\eta_{n-i}, \quad m \geq 2, n \geq m, \tag{A.17}$$

$$\psi_{i,j}^{n,m} = \frac{\partial^{i+j}}{\partial\xi_1^i \partial\xi_2^j}\left(\frac{1}{m!}\frac{\partial^m\phi_n}{\partial z^m}\bigg|_{z=0}\right), \tag{A.18}$$

$$\beta_{i,j}^{n,0} = \psi_{i,j}^{n,0}, \qquad \beta_{i,j}^{n,m} = \sum_{s=1}^{m}\psi_{i,j}^{n,s}\mu_{s,m}\epsilon_1^s \quad m \geq 1 \tag{A.19}$$

$$\gamma_{i,j}^{n,0} = \psi_{i,j}^{n,1}, \qquad \gamma_{i,j}^{n,m} = \sum_{s=1}^{m}(s+1)\psi_{i,j}^{n,s+1}\mu_{s,m}\epsilon_1^s \quad m \geq 1, \tag{A.20}$$

$$\begin{aligned}
\delta_{i,j}^{n,0} &= 2\psi_{i,j}^{n,2}, \\
\delta_{i,j}^{n,m} &= \sum_{s=1}^{m}(s+1)(s+2)\psi_{i,j}^{n,s+2}\mu_{s,m}\epsilon_1^s \quad m \geq 1,
\end{aligned} \tag{A.21}$$

$$\bar{\phi}_n^{i,j} = \sum_{m=0}^{n}\beta_{i,j}^{n-m,m}, \qquad \bar{\phi}_{z,n}^{i,j} = \sum_{m=0}^{n}\gamma_{i,j}^{n-m,m}, \tag{A.22}$$

$$\bar{\phi}_{zz,n}^{i,j} = \sum_{m=0}^{n}\delta_{i,j}^{n-m,m}. \tag{A.23}$$

It holds

$$\begin{aligned}
\mathcal{L}_1[\breve{\phi} - \phi_0] &= \frac{\partial^2(\breve{\phi} - \phi_0)}{\partial\xi_1^2} + \frac{1}{\tanh(\epsilon_1)}\frac{\partial(\breve{\phi} - \phi_0)}{\partial z} \\
&= \sum_{n=1}^{+\infty} q^n S_n,
\end{aligned} \tag{A.24}$$

where

$$\begin{aligned}
S_n &= \sum_{m=0}^{n-1}\left(\beta_{2,0}^{n-m,m} + \frac{1}{\tanh(\epsilon_1)}\gamma_{0,0}^{n-m,m}\right) \\
&= \left(\frac{\partial^2\phi_n}{\partial\xi_1^2} + \frac{1}{\tanh(\epsilon_1)}\frac{\partial\phi_n}{\partial z}\right)\bigg|_{z=0} + \bar{S}_n,
\end{aligned} \tag{A.25}$$

$$\bar{S}_n = \sum_{m=1}^{n-1}\left(\beta_{2,0}^{n-m,m} + \frac{1}{\tanh(\epsilon_1)}\gamma_{0,0}^{n-m,m}\right). \tag{A.26}$$

So, the left hand side of Eq. (A.2) becomes

$$(1-q)\mathcal{L}_1[\breve{\phi} - \phi_0] = \sum_{n=1}^{+\infty}(S_n - \chi_n S_{n-1})q^n, \tag{A.27}$$

where

$$\chi_n = \begin{cases} 0, & \text{when } n \leq 1, \\ 1, & \text{when } n > 1. \end{cases} \tag{A.28}$$

Meanwhile, the right hand side of Eq. (A.2) reads

$$\mathcal{N}_1[\breve{\phi}] = c_0\sum_{n=1}^{+\infty}\Delta_{n-1}^{\phi}q^n, \tag{A.29}$$

where

$$\Delta_m^{\phi} = \bar{\phi}_m^{2,0} + \frac{1}{\epsilon^2\tanh(\epsilon_1)}\bar{\phi}_{z,m}^{0,0} - 2\epsilon_1\Gamma_{m,1} + \epsilon_1^2\Lambda_m, \tag{A.30}$$

$$\begin{aligned}
\Gamma_{m,1} &= \sum_{n=0}^{m}(\bar{\phi}_n^{1,0}\bar{\phi}_{m-n}^{2,0} + \epsilon_3^2\bar{\phi}_n^{0,1}\bar{\phi}_{m-n}^{1,1} + \bar{\phi}_{z,n}^{0,0}\bar{\phi}_{z,m-n}^{1,0}) \\
&\quad + \epsilon_3\cos\alpha\sum_{n=0}^{m}(\bar{\phi}_n^{1,0}\bar{\phi}_{m-n}^{1,1} + \bar{\phi}_n^{2,0}\bar{\phi}_{m-n}^{0,1}),
\end{aligned} \tag{A.31}$$

$$\begin{aligned}
\Gamma_{m,2} &= \sum_{n=0}^{m}(\bar{\phi}_n^{1,0}\bar{\phi}_{m-n}^{1,1} + \epsilon_3^2\bar{\phi}_n^{0,1}\bar{\phi}_{m-n}^{0,2} + \bar{\phi}_{z,n}^{0,0}\bar{\phi}_{z,m-n}^{0,1}) \\
&\quad + \epsilon_3\cos\alpha\sum_{n=0}^{m}(\bar{\phi}_n^{1,0}\bar{\phi}_{m-n}^{0,2} + \bar{\phi}_n^{0,1}\bar{\phi}_{m-n}^{1,1}),
\end{aligned} \tag{A.32}$$

$$\begin{aligned}
\Gamma_{m,3} &= \sum_{n=0}^{m}(\bar{\phi}_n^{1,0}\bar{\phi}_{z,m-n}^{1,0} + \epsilon_3^2\bar{\phi}_n^{0,1}\bar{\phi}_{z,m-n}^{0,1} + \bar{\phi}_{z,n}^{0,0}\bar{\phi}_{zz,m-n}^{0,0}) \\
&\quad + \epsilon_3\cos\alpha\sum_{n=0}^{m}(\bar{\phi}_n^{1,0}\bar{\phi}_{z,m-n}^{0,1} + \bar{\phi}_n^{0,1}\bar{\phi}_{z,m-n}^{1,0}),
\end{aligned} \tag{A.33}$$

$$\begin{aligned}
\Lambda_m &= \sum_{n=0}^{m}(\bar{\phi}_n^{1,0}\Gamma_{m-n,1} + \epsilon_3^2\bar{\phi}_n^{0,1}\Gamma_{m-n,2} + \bar{\phi}_{z,n}^{0,0}\Gamma_{m-n,3}) \\
&\quad + \epsilon_3\cos\alpha\sum_{n=0}^{m}(\bar{\phi}_n^{1,0}\Gamma_{m-n,2} + \bar{\phi}_n^{0,1}\Gamma_{m-n,1}).
\end{aligned} \tag{A.34}$$

Thus, the high-order deformation equation on $z = 0$ for potential velocity function is

$$\bar{\mathcal{L}}[\phi_m] = c_0\Delta_{m-1}^{\phi} + \chi_m S_{m-1} - \bar{S}_m = R_{1,m}(\xi_1, \xi_2), \tag{A.35}$$

where

$$\bar{\mathcal{L}}[\phi_m] = \left(\frac{\partial^2\phi_m}{\partial\xi_1^2} + \frac{1}{\tanh(\epsilon_1)}\frac{\partial\phi_m}{\partial z}\right)\bigg|_{z=0}. \tag{A.36}$$

The high-order deformation equation for the wave elevation hence becomes

$$\eta_m = c_0\Delta_{m-1}^{\eta} + \chi_m\eta_{m-1} = R_{3,m}(\xi_1, \xi_2), \tag{A.37}$$

where

$$\Delta_{m-1}^{\eta} = \eta_{m-1} - \epsilon^2\tanh(\epsilon_1)(\bar{\phi}_{m-1}^{1,0} - \epsilon_1\Gamma_{m-1,0}), \tag{A.38}$$

$$\begin{aligned}
\Gamma_{m,0} &= \sum_{n=0}^{m}\left(\frac{1}{2}\bar{\phi}_n^{1,0}\bar{\phi}_{m-n}^{1,0} + \frac{1}{2}\epsilon_3^2\bar{\phi}_n^{0,1}\bar{\phi}_{m-n}^{0,1} + \frac{1}{2}\bar{\phi}_{z,n}^{0,0}\bar{\phi}_{z,m-n}^{0,0}\right. \\
&\quad \left. + \epsilon_3\cos\alpha\bar{\phi}_n^{1,0}\bar{\phi}_{m-n}^{0,1}\right).
\end{aligned} \tag{A.39}$$

Meanwhile, on the bottom $z = -\epsilon_1 + q(\epsilon_2/\epsilon_3)\zeta$, by expanding $\phi_n(\xi_1, \xi_2, z)$ at $z = -\epsilon_1$, we have

$$\begin{aligned}
\phi_n(\xi_1, \xi_2, z) &= \phi_n|_{z=-\epsilon_1} \\
&\quad + \sum_{m=1}^{+\infty}\left(\frac{1}{m!}\frac{\partial^m\phi_n}{\partial z^m}\bigg|_{z=-\epsilon_1}\right)q^m(\epsilon_2/\epsilon_3)^m\zeta^m,
\end{aligned} \tag{A.40}$$

$$\begin{aligned}
\frac{\partial^{i+j}\phi_n(\xi_1, \xi_2, z)}{\partial\xi_1^i\partial\xi_2^j} &= \frac{\partial^{i+j}\phi_n}{\partial\xi_1^i\partial\xi_2^j}\bigg|_{z=-\epsilon_1} \\
&\quad + \sum_{m=1}^{+\infty}\frac{\partial^{i+j}}{\partial\xi_1^i\partial\xi_2^j}\left(\frac{1}{m!}\frac{\partial^m\phi_n}{\partial z^m}\bigg|_{z=-\epsilon_1}\right) \\
&\quad \times q^m(\epsilon_2/\epsilon_3)^m\zeta^m,
\end{aligned} \tag{A.41}$$

$$\begin{aligned}
\frac{\partial\phi_n(\xi_1, \xi_2, z)}{\partial z} &= \frac{\partial\phi_n}{\partial z}\bigg|_{z=-\epsilon_1} \\
&\quad + \sum_{m=1}^{+\infty}\left(\frac{1}{m!}\frac{\partial^{m+1}\phi_n}{\partial z^{m+1}}\bigg|_{z=-\epsilon_1}\right) \\
&\quad \times q^m(\epsilon_2/\epsilon_3)^m\zeta^m.
\end{aligned} \tag{A.42}$$

Defining

$$\tilde{\psi}_{i,j}^{n,m} = \frac{\partial^{i+j}}{\partial\xi_1^i\partial\xi_2^j}\left(\frac{1}{m!}\frac{\partial^m\phi_n}{\partial z^m}\bigg|_{z=-\epsilon_1}\right), \tag{A.43}$$

then, on $z = -\epsilon_1 + q(\epsilon_2/\epsilon_3)\zeta$, we have

$$\phi_n(\xi_1, \xi_2, z) = \tilde{\psi}_{0,0}^{n,0} + \sum_{m=1}^{+\infty} \tilde{\psi}_{0,0}^{n,m} q^m (\epsilon_2/\epsilon_3)^m \zeta^m, \tag{A.44}$$

$$\frac{\partial^{i+j}\phi_n(\xi_1, \xi_2, z)}{\partial \xi_1^i \partial \xi_2^j} = \tilde{\psi}_{i,j}^{n,0} + \sum_{m=1}^{+\infty} \tilde{\psi}_{i,j}^{n,m} q^m (\epsilon_2/\epsilon_3)^m \zeta^m, \tag{A.45}$$

$$\frac{\partial^{i+j+1}\phi_n(\xi_1, \xi_2, z)}{\partial z \partial \xi_1^i \partial \xi_2^j}$$

$$= \tilde{\psi}_{i,j}^{n,1} + \sum_{m=1}^{+\infty} (m+1) \tilde{\psi}_{i,j}^{n,m+1} q^m (\epsilon_2/\epsilon_3)^m \zeta^m. \tag{A.46}$$

On $z = -\epsilon_1 + q(\epsilon_2/\epsilon_3)\zeta$, we have

$$\frac{\partial}{\partial z} \left[\breve{\phi}(\xi_1, \xi_2, z; q) - \phi_0(\xi_1, \xi_2, z) \right] = \sum_{n=1}^{+\infty} q^n T_n, \tag{A.47}$$

where

$$T_n = \tilde{\psi}_{0,0}^{n,1} + \bar{T}_n,$$
$$\bar{T}_n = \sum_{m=1}^{n-1} (m+1) \tilde{\psi}_{0,0}^{n-m,m+1} (\epsilon_2/\epsilon_3)^m \zeta^m. \tag{A.48}$$

Thus, the left-hand side of Eq. (A.4) hence becomes

$$(1-q)\mathcal{L}_2[\breve{\phi}(\xi_1, \xi_2, z; q) - \phi_0(\xi_1, \xi_2, z)]$$

$$= \sum_{n=1}^{+\infty} q^n [T_n - \chi_n T_{n-1}]. \tag{A.49}$$

Besides, we have

$$\frac{\partial \breve{\phi}(\xi_1, \xi_2, z; q)}{\partial z} = \sum_{n=0}^{+\infty} \frac{\partial \phi_n}{\partial z} q^n$$

$$= \sum_{n=0}^{+\infty} q^n \left(\sum_{m=0}^{n} (m+1) \tilde{\psi}_{0,0}^{n-m,m+1} (\epsilon_2/\epsilon_3)^m \zeta^m \right), \tag{A.50}$$

$$\frac{\partial \breve{\phi}(\xi_1, \xi_2, z; q)}{\partial \xi_1} = \sum_{n=0}^{+\infty} \frac{\partial \phi_n}{\partial \xi_1} q^n$$

$$= \sum_{n=0}^{+\infty} q^n \left(\sum_{m=0}^{n} \tilde{\psi}_{1,0}^{n-m,m} (\epsilon_2/\epsilon_3)^m \zeta^m \right), \tag{A.51}$$

$$\frac{\partial \breve{\phi}(\xi_1, \xi_2, z; q)}{\partial \xi_2} = \sum_{n=0}^{+\infty} \frac{\partial \phi_n}{\partial \xi_2} q^n$$

$$= \sum_{n=0}^{+\infty} q^n \left(\sum_{m=0}^{n} \tilde{\psi}_{0,1}^{n-m,m} (\epsilon_2/\epsilon_3)^m \zeta^m \right). \tag{A.52}$$

So, the right-hand side of Eq. (A.4) reads

$$q\, c_0\, \mathcal{N}_3[\breve{\phi}] = c_0 q \left[\frac{\partial \breve{\phi}}{\partial z} + \epsilon_2 \sin \xi_2 \left(\cos \alpha \frac{\partial \breve{\phi}}{\partial \xi_1} + \epsilon_3 \frac{\partial \breve{\phi}}{\partial \xi_2} \right) \right]$$

$$= c_0 \sum_{n=1}^{+\infty} q^n \Delta_{n-1}^b, \tag{A.53}$$

where

$$\Delta_n^b = \left[\tilde{\psi}_{0,0}^{n,1} + \epsilon_2 \sin \xi_2 \left(\cos \alpha \tilde{\psi}_{1,0}^{n,0} + \epsilon_3 \tilde{\psi}_{0,1}^{n,0} \right) \right]$$

$$+ \sum_{m=1}^{n} (\epsilon_2/\epsilon_3)^m \zeta^m \left[(m+1) \tilde{\psi}_{0,0}^{n-m,m+1} \right.$$

$$\left. + \epsilon_2 \sin \xi_2 \left(\cos \alpha \tilde{\psi}_{1,0}^{n-m,m} + \epsilon_3 \tilde{\psi}_{0,1}^{n-m,m} \right) \right]. \tag{A.54}$$

Thus, the high-order bottom condition reads

$$\bar{\mathcal{L}}_2[\phi_m] = c_0 \Delta_{m-1}^b + \chi_m T_{m-1} - \bar{T}_m$$

$$= R_{2,m}(\xi_1, \xi_2), \quad \text{on } z = -\epsilon_1, \tag{A.55}$$

where

$$\bar{\mathcal{L}}_2[\phi_m] = \left. \frac{\phi_m}{\partial z} \right|_{z=-\epsilon_1}. \tag{A.56}$$

Note that $\zeta = \cos \xi_2$ in all of above formulas.

References

[1] O. Phillips, On the dynamics of unsteady gravity waves of finite amplitude part 1. The elementary interactions, J. Fluid Mech. 9 (02) (1960) 193–217.
[2] D.J. Benney, Non-linear gravity wave interactions, J. Fluid Mech. 14 (4) (1962) 577–584.
[3] L.W. Schwartz, Computer extension and analytic continuation of Stokes' expansion for gravity waves, J. Fluid Mech. 62 (3) (1974) 553–578.
[4] M.S. Longuet-Higgins, Integral properties of periodic gravity waves of finite amplitude, Proc. R. Soc. A 342 (1629) (1975) 157–174.
[5] S.J. Liao, K.F. Cheung, Homotopy analysis of nonlinear progressive waves in deep water, J. Engrg. Math. 45 (2) (2003) 105–116.
[6] P.A. Madsen, D.R. Fuhrman, Third-order theory for multi-directional irregular waves, J. Fluid Mech. 698 (2012) 304–334.
[7] S.J. Liao, Proposed homotopy analysis techniques for the solution of nonlinear problems (Ph.D. thesis), Shanghai Jiao Tong University, 1992.
[8] S.J. Liao, Beyond Perturbation: Introduction to the Homotopy Analysis Method, CRC Press, Boca Raton, 2003.
[9] S.J. Liao, A uniformly valid analytic solution of 2D viscous flow past a semi-infinite flat plate, J. Fluid Mech. 385 (1999) 101–128.
[10] S.J. Liao, On the analytic solution of magnetohydrodynamic flows of non-Newtonian fluids over a stretching sheet, J. Fluid Mech. 488 (2003) 189–212.
[11] S.J. Liao, Homotopy Analysis Method in Nonlinear Differential Equations, Springer & Higher Education Press, Heidelberg, 2012.
[12] S. Abbasbandy, Homotopy analysis method for heat radiation equations, Int. Commun. Heat Mass Transfer 34 (3) (2007) 380–387.
[13] K. Vajravelu, R. Van Gorder, Nonlinear Flow Phenomena and Homotopy Analysis, Springer & Higher Education Press, Heidelberg, 2013.
[14] S.J. Liao, On the homotopy multiple-variable method and its applications in the interactions of nonlinear gravity waves, Commun. Nonlinear Sci. Numer. Simul. 16 (3) (2011) 1274–1303.
[15] D.L. Xu, Z.L. Lin, S.J. Liao, M. Stiassnie, On the steady-state fully resonant progressive waves in water of finite depth, J. Fluid Mech. 710 (2012) 379–418.
[16] Z. Liu, S.J. Liao, Steady-state resonance of multiple wave interactions in deep water, J. Fluid Mech. 742 (2014) 664–700.
[17] Z. Liu, D.L. Xu, J. Li, T. Peng, A. Alsaedi, S.J. Liao, On the existence of steady-state resonant waves in experiment, J. Fluid Mech. (2014). http://dx.doi.org/10.1017/jfm.2014.658.
[18] A.D. Heathershaw, Seabed-wave resonance and sand bar growth, Nature 296 (1982) 343–345.
[19] A.G. Davies, A.D. Heathershaw, Surface-wave propagation over sinusoidally varying topography, J. Fluid Mech. 144 (1984) 419–443.
[20] J.T. Kirby, General wave equation for waves over rippled beds, J. Fluid Mech. 162 (1986) 171–186.
[21] P.G. Chamberlain, D. Porter, The modified mild-slope equation, J. Fluid Mech. 291 (1995) 393–407.
[22] Y. Liu, D.K.P. Yue, On generalized Bragg scattering of surface waves by bottom ripples, J. Fluid Mech. 356 (1998) 297–326.
[23] J. Miles, On gravity-wave scattering by non-secular changes in depth, J. Fluid Mech. 376 (1998) 53–60.
[24] Y.S. Cho, C. Lee, Resonant reflection of waves over sinusoidally varying topographies, J. Coast. Res. 16 (3) (2000) 870–876.
[25] C.C. Mei, Resonant reflection of surface water waves by periodic sandbars, J. Fluid Mech. 152 (1985) 315–335.
[26] F. Ardhuin, T.H.C. Herbers, Bragg scattering of random surface gravity waves by irregular seabed topography, J. Fluid Mech. 451 (2002) 1–33.
[27] F. Ardhuin, R. Magne, Scattering of surface gravity waves by bottom topography with a current, J. Fluid Mech. 576 (2007) 235–264.
[28] J. Yu, C.C. Mei, Do longshore bars shelter the shore? J. Fluid Mech. 404 (2000) 251–268.
[29] J. Yu, L. Howard, Exact floquet theory for waves over arbitrary periodic topographies, J. Fluid Mech. 712 (2012) 451–470.
[30] A. Mitra, M.D. Greenberg, Slow interactions of gravity waves and a corrugated sea bed, J. Appl. Mech. 51 (1984) 251–255.
[31] A.G. Davies, Some interactions between surface water waves and ripples and dunes on the seabed, 1980, http://eprints.soton.ac.uk/14524/1/14524-01.pdf.
[32] C.C. Mei, M. Stiassnie, D. Yue, Theory and Applications of Ocean Surface Waves: Nonlinear Aspects, Vol. 2, World Scientific, 2005.
[33] W.H. Bragg, W.L. Bragg, X Rays and Crystal Structure, Bell, 1915.